Results in Engineering 30 (2026) 111083

Contents lists available at ScienceDirect

Results in Engineering

journal homepage: www.sciencedirect.com/journal/results-in-engineering

Research paper

Hybrid renewable energy systems in educational institutions: Pathways to sustainability and cost-effectiveness

Asjad Ali [a], Noor Izzri Abdul Wahab [a], Zain Ul Abdeen Qureshi [b,c], Usama Azmat [d], Hafiz Abdul Muqeet [e], Reihaneh Aghamolaei [f,*]

[a] Advanced Lightning Power and Energy Research (ALPER), Department of Electrical and Electronic Engineering, Faculty of Engineering, Universiti Putra Malaysia, 43400, UPM, Serdang, Selangor, Malaysia
[b] Department of Electrical and Computer Engineering, Faculty of Engineering, King Abdulaziz University, Jeddah 21589, Saudi Arabia
[c] U.S.-Pakistan Centre for Advanced Studies in Energy (USPCAS-E), National University of Sciences and Technology (NUST), H-12, Islamabad 44000, Pakistan
[d] University of Gujrat Sub campus Mandi Bahauddin Department of Physics, University of Gujrat, 50400 Mandi Bahauddin, Pakistan
[e] Department of Electrical Engineering Technology, Punjab Tianjin University of Technology, Lahore 54770, Pakistan
[f] School of Mechanical and Manufacturing Engineering, Faculty of Engineering and Computing, Dublin City University, Whitehall, Dublin 9, Ireland

ARTICLE INFO

Keywords:
Hybrid renewable energy system
Renewable energy sources
Homer Pro
Net present cost
Educational institutes
Carbon emission
Techno-economic analysis

ABSTRACT

Hybrid renewable energy systems offer a cost-effective solution for meeting the energy demands of educational institutions, particularly when both academic and non-academic loads are considered. Unlike most existing studies that focus only on academic buildings, this research incorporates a comprehensive campus load profile, including hostels and faculty housing, enabling a more realistic assessment of university energy demand. The study develops and evaluates different hybrid energy system configurations mixing grid power, photovoltaic solar, wind, battery energy storage systems, fuel cells, electrolyzers, and hydrogen storage. Seven system configurations are developed and analysed using detailed techno-economic, environmental, and robustness assessments to identify an optimal solution that balances, sustainability, reliability and cost. The results indicate that a hybrid system that integrates grid supply, solar PV, battery storage, fuel cells, an electrolyzer, and hydrogen storage (Scenario VII) provides the most economically viable solution. This configuration has the lowest net present cost of $32.18 million and a levelised cost of energy of $0.0751/kWh, and it reduces the CO_2 emissions by 64.37% as compared to base-line gird-based scenario. Robustness analysis confirms that Scenario VII can effectively manage the load variations and ensure a reliable energy supply. Furthermore, hydrogen-based scenarios VI and VII demonstrate the potential for low-cost hydrogen production, with the levelised hydrogen costs of $5.15/kg and $2.59/kg respectively. Notably, the achieved LCOH of $2.59/kg in Scenario VII serves as a benchmark for economically viable green hydrogen production in campus-scale hybrid systems in developing countries. Overall, the findings demonstrate the potential of hybrid renewable energy systems to provide a reliable, affordable, and low-carbon energy solution for educational institutions.

1. Introduction

To achieve the goals of Paris agreement of 2015, COP 28, COP 29, and to meet the global energy consumption due to acceleration in AI race, robotics, and rapid automation, distributed energy resources (DERs) and renewable energy sources (RES) are being widely adopted

Abbreviations: HOMER, Hybrid optimization of multiple energy resources; HRES, Hybrid renewable energy system; RES, Renewable energy sources; HES, Hybrid energy systems; DERs, Distributed energy resources; WTs, Wind turbines; PV, Photovoltaics; BESS, Battery energy storage systems; LOCE, Levelised cost of energy; NPC, Net present cost; LCOH, Levelised cost of hydrogen; EMS, Energy management system; GHG, Greenhouse gas; DG, Diesel generator; HT, Hydrogen tank; FC, Fuel cell; UETT, University of engineering and technology taxila; CC, Cycle charging; SAIDI, System average interruption duration index; LF, Load following; IESCO, Islamabad electric supply company; IC, Investment cost; TNPC, The net present cost; F_lC, Fuel cost; O&M, Operation and maintenance; i_r, Is the interest rate; T_y, Time in years; CRF, Capital recovery factor; i', Nominal discount rate; f, Inflation rate; E_{DG}, Emission of gases; UL, Unmet load; STP, Standard temperature and pressure; η_{chg}, Charging efficiency; η_{dch}, Discharging efficiency; DOD $_{batt}$, Depth of discharge; Cp $_{batt}$, Capacity of the battery; RE, Renewable energy.

* Corresponding author.
E-mail addresses: abdul.muqeet@uettaxila.edu.pk (H.A. Muqeet), reihaneh.aghamolaei@dcu.ie (R. Aghamolaei).

https://doi.org/10.1016/j.rineng.2026.111083
Received 25 January 2026; Received in revised form 1 April 2026; Accepted 15 May 2026
Available online 16 May 2026

worldwide. The main goals of this transformation towards renewable resources based energy systems are to reduce carbon emissions and promote sustainable energy systems [1–3]. In addition to this, fossil fuel resources are depleting at higher rates, and are estimated to reduce significantly in the next 50 to 100 years [4,5]. HRESs are now a more appealing and practical option both technically and economically as a result of the recent significant decline in the cost of RESs and BESS. Wind turbines (WTs) and PV systems are being accepted and utilized to meet the load demands as a substitute for fossil fuel-based energy systems. Recent reports have indicated a very fast pace in the deployment of WTs and PV systems across Europe, Australia, and other developed nations to combat with endangering climate issue [6–8].

Increasing population, techno-economic and social development put further strain on developing countries to meet the rising energy demand. In Pakistan's energy mix, there is still a considerable share of fossil fuels. Until the 1980s, Pakistan was able to meet its energy demand using hydropower; however, as the population kept growing, coal and natural gas-based power plants were established. Dependence on imported oil and natural gas has persistently grown. Even today, the share of renewable-based energy sources is very low, as depicted in Fig. 1 [9,10]. Moreover, for this case study in the selected location in Pakistan, there is much work to be done on the distribution and transmission sector to enhance its energy-carrying capacity. As a result, developing countries face severe energy outages, which necessitate exploration of other feasible solutions to fulfil the energy deficits [11–13]. Conventionally, diesel generators (DGs) are deployed for contingency situations in both off-grid and on-grid configurations to meet the energy demands. The recent surge in inflation has increased the prices of fuel, making diesel-based energy solutions expensive and non-feasible for energy generation. Moreover, the diesel-based energy system releases hazardous pollutants, degrading the quality of the air and polluting the environment. Severe and scheduled energy outages disturb the academic activities in educational institutions [14–16]. Educational institutions, especially large universities, are unique energy consumers because they integrate different types of loads within a single connected facility.

In addition to classrooms, laboratories, libraries, and administrative offices that mainly operate during the day, universities also provide accommodation for students, housing for faculty, and services available on campus, such as cafeterias, sports complexes, and medical centres, which generate a significant and continuous residential load. This combination generates an intricate and a mixed load profile that entails notable fluctuations between day and night, seasonal variations, and high peak demands [17–19]. It becomes necessary to ensure the smooth availability of power in those environments, as even a brief outage can affect the daily life of thousands of residents, halt research in laboratories, damage sensitive equipment, and affect classroom activities. Pakistan's historical dependence on diesel generators, due to high fuel prices and frequent and prolonged blackouts, is harmful to the environment and economically unsustainable [20–22]. Although BESSs are effective for short-term energy balancing and intra-day load shifting, their economic and technical feasibility declines when extended-duration or seasonal storage is required. University campuses exhibit variable demand patterns and experience seasonal fluctuations in renewable energy generation, particularly due to high summer solar output and comparatively lower winter availability. In such cases, batteries are primarily suited for hourly cycling and peak shaving but are not economically optimal for storing large quantities of surplus energy over extended periods. Hydrogen storage, produced through electrolysis using excess renewable energy, offers a viable long-duration storage solution with higher energy density and minimal self-discharge over time. By integrating hydrogen storage with fuel cell conversion, the system enables seasonal energy shifting, reduces renewable curtailment, and enhances overall energy security. Therefore, the inclusion of hydrogen storage in the proposed campus hybrid system addresses limitations inherent to battery-only configurations. To fill the above-mentioned gaps in the literature review, the specific objectives of this study are to:

- Design and model a campus-scale hybrid renewable energy system integrating PV arrays, wind turbines, BESS, and auxiliary backup units to meet residential and educational load demands.
- Optimize the system configuration to achieve minimum LCOE while satisfying predefined reliability constraints.
- Utilize excess solar generation for hydrogen production and evaluate hydrogen storage as an alternative long-term energy storage solution.
- Assess the techno-economic feasibility of using stored hydrogen in a fuel cell for additional electricity generation.
- Evaluate the system's performance in terms of reliability enhancement, fossil fuel reduction, and economic viability in a developing-country context.

Recent exploration of the literature review has unveiled that there are various configurations of HRESs that have been adopted by the researchers to find a feasible solution to diminish both costs and environmental impacts. Solar PV, Wind, and BESS have been found to be the

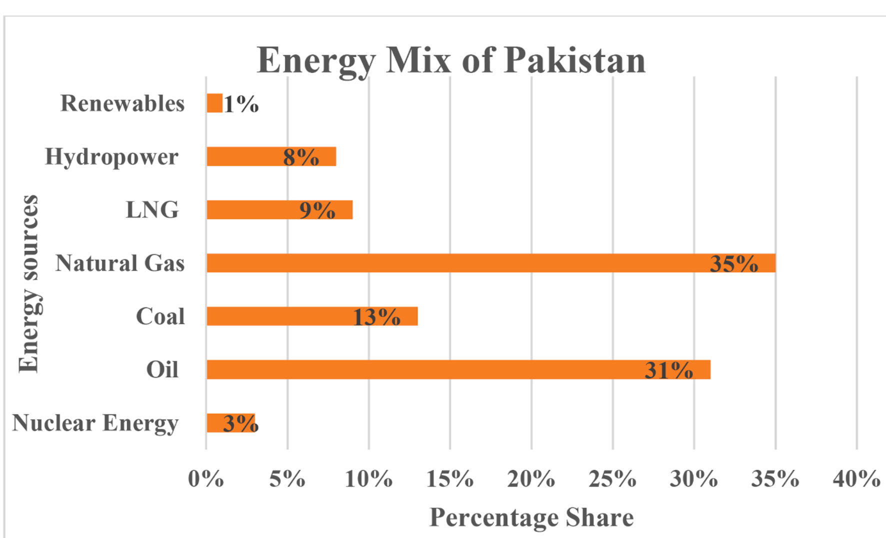

Fig. 1. Share of different energy sources in Pakistan [81].

most common configuration that is embraced by researchers for designing energy systems for remote areas, buildings, and communities [23–25]. There are a few articles that are available that have targeted the educational institutions and designed energy systems for educational institutions for different locations around the World for meeting the load demand of campuses [4,26–30].

Given the high rate of power outages, rising inflation, and fuel costs, an HES is a more feasible option for university campuses in developing nations. Nevertheless, a few studies have been conducted on HRES designs for such contexts that take into account a variety of factors, including sensitivity analysis, net metering, planned energy outages, skyrocketing inflation rates, decreased LCOE, NPC, and the role of campuses in environmental degradation [31–33]. In ref [34], the authors designed an HES consisting of solar panels, BESS, and grid energy for an AJK university located in Muzaffarabad, Pakistan. The region faces severe weather conditions and frequent outages, which cause financial losses and hinder educational activities. Therefore, the authors designed an HES to reduce LCOE as well as deal with the outage issue. The designed system reduced LCOE owing to better usage of solar energy. The results showed that the system consisting of PV/BESS/Grid was more stable, cost-efficient, and effective. However, this study did not integrate net metering into the system and only evaluated a portion of the load, and it ignored a comprehensive analysis.

In the investigation [35], an EMS system is designed that integrates PV panels, WTs, and BESS for university microgrid. The simulations are performed in MATLAB which reduced LCOE and CO_2 emissions. However, the study ignored a detailed sensitivity analysis to study the effects of different parameters. Reference [36] designed a hybrid solar photovoltaic–wind system for a university campus in Sumatra with tsunami risk using HOMER, including grid backup for lower renewable generation. Initially, battery storage was included, but it was removed after being proven economically inefficient. The final combination (62% PV, 20% wind) reduced the LCOE by 25% and supplied 82% of the campus demand. However, no sensitivity analysis was performed for the LCOE and NPC. Reference [37] designed a PV + BESS microgrid connected to the grid for Ripah International University (Lahore) using HOMER to reduce costs. The optimal system achieved 99.3% renewable energy penetration, with an NPC of $0.483M, and showed better performance compared to grid-only/diesel options. However, it ignored the sensitivity analysis (capacity reduction) and did not assess the effects of a grid blackout on the LCOE and NPC.

Reference [38] modelled in HOMER two standalone options and two grid-connected ones for the JNTUK-UCEV campus, selecting as the best a grid-connected PV–wind–diesel generator hybrid. This system generates 1,127,549 kWh of energy, with an energy mix coming from PV (64.5%), wind (1.07%), and the grid (34.4%), and emits 245,423 kg/year of CO_2 and 1,064 kg/year of SO_2. However, it did not include sensitivity analysis or grid blackout evaluation. Reference [39] designed a cost-effective DC microgrid for a rural school in Ethiopia, achieving a 51% cost reduction by using standard and high-efficiency devices. But it did not include sensitivity analysis or key factors (such as the proportion of renewable energy, capacity shortfall, or the effects of inflation on LCOE/NPC), nor did it evaluate environmental impacts. In ref [40], HOMER Pro was used to evaluate an off-grid solar–battery system with diesel backup for a remote site in northern Bangladesh (~10 kWh/day). The results showed that the LCOE decreased by more than 29% and GHG emissions were reduced by more than 69%. However, the techno-economic assessment did not adequately include the NPC and sensitivity effects.

In ref [41], a PV-Wind-BESS microgrid was evaluated for an urban university campus in order to improve reliability and reduce the NPC. By combining renewable energies with grid backup, the LCOE was reduced by approximately 50%. A sensitivity analysis (e.g., solar tracking) was included, but only a limited number of parameters were considered. Reference [42] designed a hybrid PV-wind-biomass HES for a university in Cyprus, comparing cases with and without BESS, and optimizing the size of the pumped hydro/BESS using a generalized reduced gradient algorithm. This system provided a renewable share of 99% and an energy supply of 98%, with an LCOE of $0.1626/kWh. However, it did not perform a sensitivity analysis or consider capacity shortage. Reference [43] proposed an EMS for a university campus in Pakistan using solar PV, diesel generator, and BESS to reduce LCOE and costs. This configuration showed a daily LCOE reduction and significant GHG cuts. However, it lacked a detailed technical-economic sensitivity analysis on NPC and LCOE.

Reference [44] analysed PV–grid–BESS options in the Aligarh Muslim University to reduce the LCOE using HOMER and found that PV + grid is the most economical option. The inclusion of BESS increased the LCOE by more than 60% compared to the existing system, while PV + grid significantly reduced environmental pollution (CO_2, SO_2, NOx). However, grid outages and electricity interruptions were not considered. Reference [45] evaluated solar/wind-based systems for university systems in the states of Nigeria using 24 years of NASA resource data and found that hybrid renewable energies generally perform better than individual options, depending on the location. The LCOE and NPC vary with changes in resources, but this study ignored capacity shortages, limits on the proportion of renewable energies, and electricity outage conditions. Reference [46] designed microgrids consisting solely of solar panels (1.5 megawatts), solely of wind, and hybrid solar-wind for the University of Medina. In the best case, an LCOE of approximately $0.051/kWh was achieved (with a payback period of 18.6 years), while the wind and hybrid cases had paybacks of 23.6 and 20.7 years, respectively, with approximately $0.064 and $0.061/kWh. A significant reduction in emissions was achieved, but lack of capacity and grid failure conditions were not considered (Table 1).

1.1. Contributions of the study

The basic purpose of this study is to develop a sustainable and cost-efficient Hybrid Energy System. Considering the gaps in the literature review and the purview of the current study, the major contributions of the study are given as;

- In the study of educational institutes, usually, academic load is considered in literature, while the other associated loads with the university, consisting of hostels and faculty housing, are ignored. In this study, both loads are considered and calculated for precise load estimation.
- In this work, hybrid energy systems including PV/Wind/Grid/BESS/FC integrated with electrolyzer and HT are developed, and a detailed techno-economic, environmental, social, and robustness analyses are conducted for determining optimal configuration for sustainable and cost-efficient energy supply considering Pakistani Energy Supply and frequent grid outages. Seven configurations consisting of various energy sources are developed, and the most optimal configuration is determined based on the sustainable and clean energy supply, reliability of the configuration in case of usual load variations, and related expenses with each configuration. Though some systems are found to be highly environmentally feasible, an optimal configuration is determined based on a trade-off between costs, the system's robustness, and environmental feasibility.
- Once the optimal configuration is determined, a comprehensive sensitivity analysis is conducted to assess how variations in multiple parameters influence NPC and LCOE.

Table 1
Major findings and limitations of previous studies.

Ref	Type of Area	Application Area	Software	Grid	DG	PV	Wind	BESS	Electrolyzer	HT	FC	Connected Load Type		Sensitivity Parameters								Investigated Results			
												Commercial Load	Residential Load	Solar Irradiance	Inflation Rate	Project Life Time	Solar Reserves	Discount Rate	Temperature	Capacity Shortage	Peak Load Reserves	PV Derating Factor	LCOE	NPC	Emission analysis
[34]	University campus	Grid Connected	HOMER	✔	×	✔	×	✔	×	×	×	✔	×	×	×	×	×	×	×	×	×	×	✔	✔	✔
[35]	University campus	Grid Connected	MATLAB	✔	×	✔	✔	✔	×	×	×	✔	✔	×	×	×	×	×	×	×	×	×	✔	✔	✔
[36]	University campus	Grid Connected	MATLAB	✔	×	✔	✔	✔	×	×	×	✔	×	×	×	×	×	×	×	×	×	×	✔	✔	✔
[37]	University campus	Grid Connected	HOMER	✔	✔	✔	×	✔	×	×	×	✔	×	×	×	×	×	×	×	×	×	×	✔	✔	✔
[86]	Hospital Area	Grid Connected/ Off-Grid	HOMER	✔	✔	✔	×	✔	×	×	×	✔	×	×	×	×	×	×	×	×	×	✔	✔	✔	✔
[65]	Residential Area	Grid Connected	HOMER	✔	✔	✔	✔	×	×	×	×	×	✔	✔	×	×	×	×	✔	×	×	×	✔	✔	✔
[87]	Microgrid	Off-Grid	HOMER	×	×	✔	✔	✔	✔	✔	✔	×	×	✔	✔	✔	×	✔	×	✔	×	×	✔	✔	✔
[88]	University campus	Grid Connected/ Off-Grid	HOMER	✔	✔	✔	✔	✔	×	×	×	✔	✔	✔	×	×	×	×	×	×	×	×	✔	✔	✔
[89]	University campus	Grid Connected/ Off-Grid	HOMER	✔	✔	✔	✔	✔	✔	✔	×	×	×	×	×	×	×	×	×	×	×	×	✔	✔	✔
[90]	Microgrid	Off-Grid	HOMER	×	✔	✔	✔	✔	×	×	×	×	✔	×	×	×	×	×	×	×	×	×	✔	✔	✔
[91]	Microgrid	Off-Grid	HOMER	✔	×	✔	×	✔	✔	✔	×	×	×	×	×	×	×	×	×	×	×	×	✔	✔	✔
[92]	Microgrid	On-Grid	HOMER MATLAB	✔	×	✔	×	✔	✔	✔	✔	×	×	×	×	×	×	×	×	×	×	✔	✔	✔	✔
[93]	Microgrid	On-Grid	HOMER	✔	×	✔	×	×	×	×	×	×	×	✔	×	×	×	×	✔	×	×	×	✔	✔	✔
Present Study	University Campus	On-Grid	HOMER	✔	✔	✔	✔	✔	✔	✔	✔	✔	✔	✔	✔	✔	✔	✔	✔	✔	✔	✔	✔	✔	✔

The rest of the article is presented in the following manner. Section 3 describes the methodology adopted in the study. Section 2 included a detailed evaluation of available resources; a comprehensive calculation of load was performed along with mathematical modelling of different components. Section 3 presents result of the study. It describes the different types of analysis that have been undertaken in this study for detailed analysis. Section 4 provides a detailed discussion and policy implications for concerned authorities, and an optimal system is also selected based on the analysis in Section 3. Section 5 provides the conclusion, limitations of the conducted study, and future recommendations.

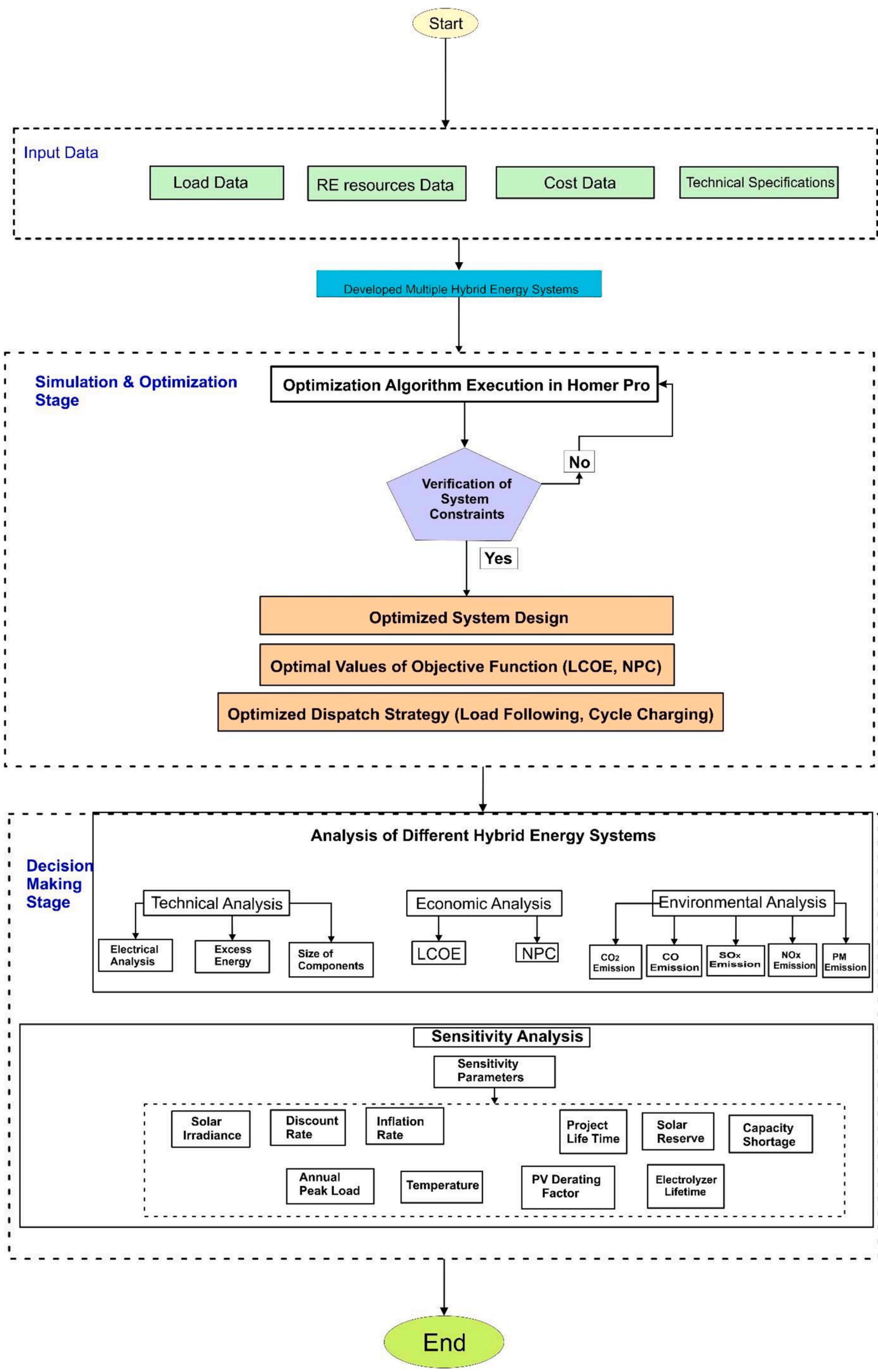

Fig. 2. Flow chart of methodological approach undertaken in the Study.

2. Methodology

This work aims to present an HRES for the load profile of a university campus. Therefore, the methodology of this study consists of multiple steps. To benefit from the available energy sources, the HRES must be designed with techno-economic perspectives and with a framework for hybrid configuration of the energy systems. Fig. 2 presents the methodological approach that has been undertaken to conduct this study. This study consists of three major phases. The first stage is called the preliminary stage, and it aids in determining the load demand of the selected location and available energy resources.

In the preliminary stage of the study, the University of Engineering and Technology, Taxila (UETT) was chosen as the site to be studied for this study. At the initial stage, daily load data was collected from the university management, and a comprehensive load assessment was converted into observable load data. The University campus is located in a far-flung location from the main city, where there are no significant topographical or urban obstacles, thereby reducing local variability. Owing to non-availability of long-term specific solar irradiance, wind speeds, and temperature data, the NASA ground meteorology and solar energy databases were chosen, as they provide an averaged datasets over 22 years, that are reliable and have proven to be useful in global coverage studies and hybrid energy systems. This approach ensures the assessment of resources to be consistent and comparable while keeping the implementation within the scope of the study. The search space constraints used for different components and energy resources in different scenarios are presented in Table A14 in the appendix section.

A DG is also chosen as a non-renewable energy source. The HRES model was designed using the components available in the Homer Pro software. Detailed data regarding the cost of the individual components, their technical specifications, and economic values are also utilised for designing an optimised HRES. The modelling of the HRES was carried out using the prices of components from literature, which are cited in the subsequent sections, with an age of 25 years, a nominal discount rate of 8%, an expected inflation rate of 8% estimated by the State Bank of Pakistan (SBP), and a BESS lifetime of 5 years. Variations in the estimates of the LCOE and NPC were adjusted based on alternative prices to provide a real economic assessment.

The assumptions undertaken for this study are presented in Table D in the appendix section. In this method, both load following (LF) and Cycle charging (CC) strategies are employed to optimise different hybrid energy systems based on LCOE, NPC, and CO_2 emissions. The CC maximizes the generator's production during operation to quickly charge the batteries, increasing autonomy during low renewable cycles. LF emphasizes renewable generation for the immediate supply of load, which reduces fuel use. These strategies allow for a sensitivity analysis of the effects on the technical and economic performance of control decisions, and reflect general and conflicting methods in the operation of hybrid systems. It should also be noted that PV capacity is not sized solely to match campus electricity demand. Instead, the optimization considers the campus as an integrated energy hub, where excess PV generation can be directed toward battery storage, electrolyzer operation, and grid export. Therefore, the resulting PV capacities reflect techno-economic optimization under multi-objective criteria (cost minimization, renewable integration, hydrogen production, and reliability enhancement), rather than simple load-matching design.

After the HRES modelling, in the optimization phase, sensitivity and optimization analyses are performed for a comprehensive evaluation. To ensure the techno-economic viability of the designed system, HOMER software takes into account both technical and economic aspects, including factors such as sizing of components involved in the design, energy generation, costs, miscellaneous expenses, and various financial parameters. In the decision-making phase, the results are verified, and the best energy systems are identified. At this stage, all analyses related to the sustainability of the design for the selected area are carried out, including power supply, costs, expenses, efficiency, and sensitivity assessments.

2.1. Calculation of resource availability, spatial analysis, load estimation, and description of the hybrid energy system framework

This section covers resource availability, spatial analysis, and load estimation calculations for the hybrid energy system. It presents a scheme of the methods used to estimate renewable energy capacity and load demands. The hybrid energy system framework is then described, detailing its components and their integration.

2.1.1. Assessment of solar irradiance, wind speeds, and temperature

For the correct simulation and analysis of hybrid renewable energy systems, reliable information on solar and wind resources is needed. This study uses HOMER software to estimate average solar radiation and wind speed, which includes integrated datasets from the NASA database [47]. Since on-site measurements are often not available, NASA satellite data can make resource modelling in different locations consistent and reliable. HOMER Pro collects average monthly values of solar radiation, wind speed, temperature, and clearness index. For the selected site, the average annual solar radiation is approximately 4.89 kWh/m^2/day, and the average wind speed is about 3 meters per second. The monthly variations of these factors are shown in Fig. 3 (a) and (b).

During the summer, solar radiation reaches its peak, providing the best conditions for solar energy generation, while wind speed remains constant throughout the year. Temperature variations are greater in June and smaller in January, indicating favourable conditions for hybrid energy systems. Although the NASA POWER dataset is widely used to assess renewable resources, its spatial resolution ($\sim 0.5^\circ \times 0.5^\circ$) cannot fully capture local factors such as shading, temperature, and seasonal irregularities. Without local on-site measurements, the results may have moderate biases.

2.1.2. Load assessment

The electrical load is monitored hourly for the university's departments and residential areas, including dormitories. For analysis, the loads of the residential areas and dormitories are combined into a single load profile. The maximum load for the university departments is 901.7 kilowatts, while the average daily consumption is 5,165 kilowatt-hours. In comparison, the maximum load for the combined residential areas and dormitories is 750.65 kilowatts, and the average daily consumption is 8,550 kilowatt-hours. During the summer months (June, July, and August), the maximum load is recorded due to increased air conditioning use. During the winter months (October to January), higher consumption is also observed due to heating needs.

In the academic departments, energy consumption occurs from 8:00 a.m. to 4:00 p.m. due to laboratory equipment, which includes computers, projectors, and specialized lab equipment. In auditoriums, electricity is required for lighting, multimedia systems, and air conditioning in the summer, and for heating in the winter. Administrative offices contribute to the load due to computers, printers, and other office equipment. In residential areas and dormitories, the highest load shifts to the afternoon (from 5:00 p.m. to 12:00 a.m.) when students return from their educational activities. Along with lighting and personal electronic devices, the load in dormitories and residential areas also includes kitchen appliances such as microwaves and electric stoves.

During the winter months, heating systems significantly increase energy demand, as during the peak of winter, the temperature can drop to 10°C. These heating systems, along with water heaters and other appliances, increase energy consumption, especially in the afternoon when residents use them the most. This seasonal change contributes to the campus's variable load profile. Detailed calculations of the load of various components and operating schedules are presented in Tables A3, A4, and A5 of the appendix.

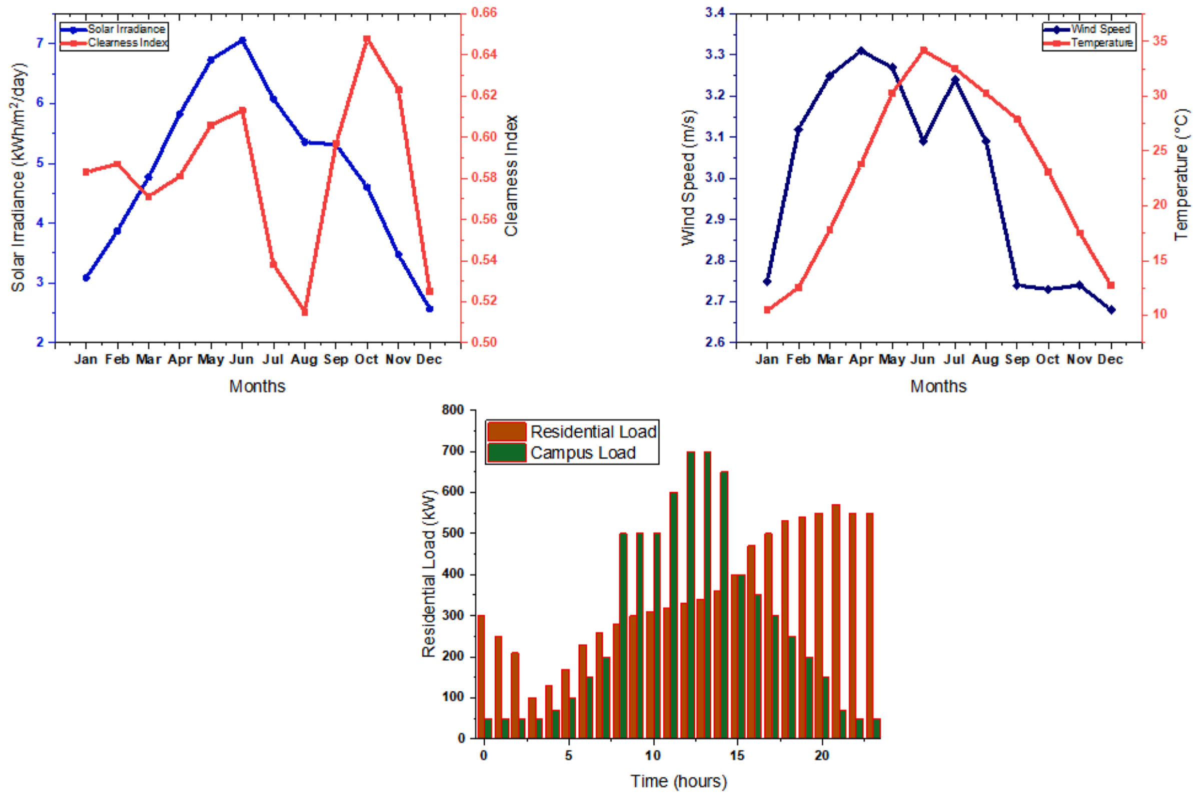

Fig. 3. (a) Average monthly solar irradiance and clearness index (b) Average monthly temperature & wind speeds (c) Load patterns.

2.1.3. *Spatial analysis*

This research is based at the UETT located in the city of Taxila, Pakistan (33°46′01.46″N, 72°49′25.71″E). The main campus includes academic faculties, student dormitories, and residential colonies. With the ongoing construction of new departments and residences, a significant increase in energy demand on campus is expected by 2027. Currently, electricity is supplied by the Islamabad Electric Supply Company (IESCO), and in the event of power outages, a 600-kW DG is available as backup [48]. As shown in Fig. 3, the average solar irradiance ranges from approximately 2.5 to 7.1 kWh/m^2/day, with peak values observed during May and June. The clearness index reaching nearly 0.65 further indicates high solar availability throughout the year.

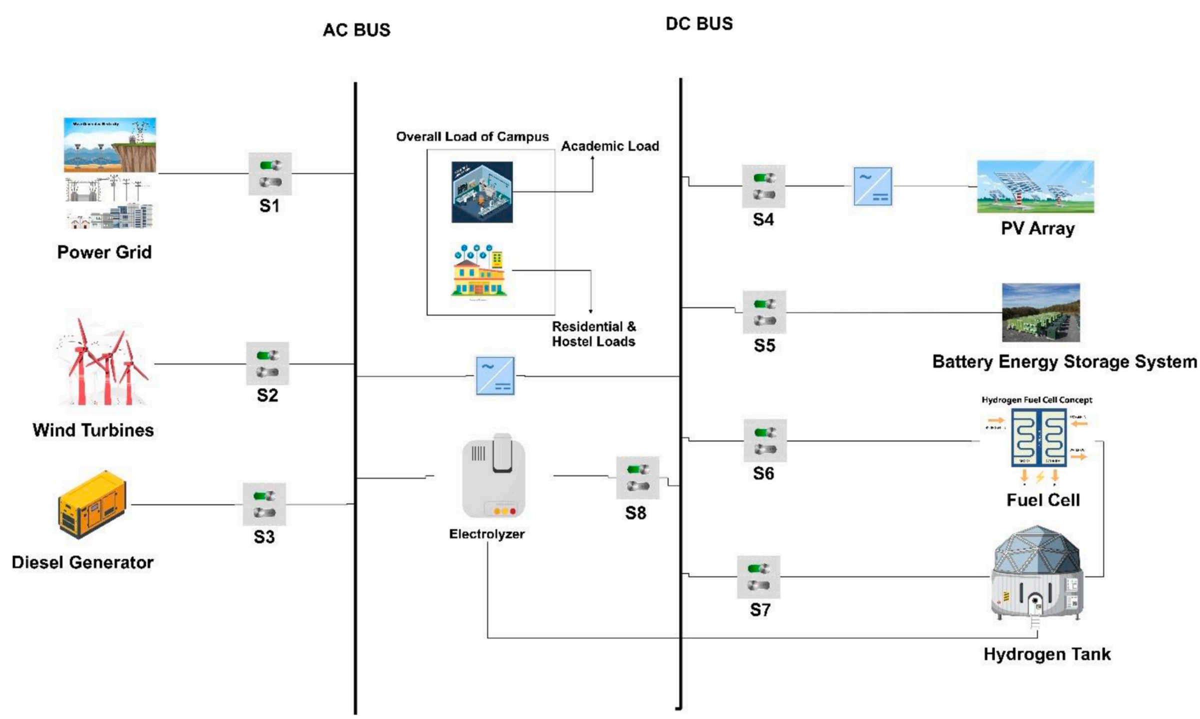

Fig. 4. Structure of designed hybrid energy systems.

Such solar intensity is sufficient to generate substantial daytime power from PV arrays, particularly during peak summer months when generation can exceed instantaneous campus demand. This seasonal and diurnal surplus energy creates a practical opportunity for hydrogen production via electrolysis. By converting excess solar energy into hydrogen and storing it for later use in a fuel cell, the system can reduce renewable energy curtailment while enhancing reliability. Therefore, the strong solar resource characteristics of UETT directly support the technical feasibility of integrating hydrogen production within the proposed hybrid system.

2.1.4. Description of hybrid energy system framework

The proposed study includes several components, such as PVs, WTs, BESS, FCs, DG, electrolyzers, and a HTs, which are organized into different hybrid renewable energy systems. In various scenarios, these components are systematically incorporated or excluded to create a unique system. This flexible and modular approach helps comprehensively assess the technical performance, economic feasibility, and environmental impacts of each configuration. By changing the presence of the components in different scenarios, the study identifies the best configuration for a reliable, cost-effective, and sustainable energy supply. The switching logic that manages the inclusion of each component in each scenario is described in Table A1 and Fig. 4 presents visual representation of the system.

2.2. Theoretical framework (Key Performance Indicators)

The objective function that defines the problem formulation and the constraints remain constant and unchanged. The main goal of this research is to design a configuration with a lower LCOE, NPC, and emissions. HOMER evaluates all renewable energy system configurations and analyzes the NPC during the simulation.

2.2.1. Net present cost

This NPC represents the total cost of the project, including the initial investment, operational and maintenance expenses, and calculates all cash flows over the system's useful life. HOMER calculates the NPC for each component and the overall system [49].

$$\text{The Net Present Cost (TNPC)} = IC + F_lC + O\&M + R_pC \tag{1}$$

Eq. 1 defines IC as the investment cost, F_lC as fuel cost, O&M as operation and maintenance cost, and R_pC as replacement cost [49].

2.2.2. Levelised cost of energy

The Levelized Cost of Energy (LCOE) represents the average cost of usable energy per kilowatt-hour over the system's life, indicating the minimum price to recover project costs. It compares the cost efficiency of different energy systems. HOMER calculates LCOE by relating the annual energy cost to the usable electricity generated, using the net annual cost divided by the total annual electrical energy $E_{total}(t)$. This metric reflects the per-unit price of energy from different sources [50].

$$LCOE = \frac{C_{total}}{\sum_{t=1}^{8760} E_{total}(t)} \tag{2}$$

Eq. A1 in the appendix section can be used to find the total annual energy cost of the system. The capital recovery factor can be determined from Eq. A2 in the appendix section [51–53].

2.2.3. Unmet load

The unmet load is calculated using Eq. 3, where total energy supplied to the consumer is divided by the total required load. It is one of the imperative key parameters because there is a huge parity between the load supply and demand, this can jeopardize the system reliability, therefore determining this for each designed system is necessary.

$$\text{Unmet Load (UL)} = \frac{\text{Total supplied load in a year}}{\text{Total Required Load}} \tag{3}$$

2.2.4. Real discount rate

The real discount rate is used to convert one-time costs into equivalent annual costs, allowing for accurate economic comparisons over time. In HOMER Pro, it is calculated according to the following formula using the nominal discount rate (i') and the inflation rate (f).

$$i = \frac{i' - f}{i + f} \tag{4}$$

2.2.5. Emission

Eq. 5 is used to calculate the emission of gases. For the DG, the emission of gases can be calculated as

$$E_{DG} = F_{DG}.\ EF_{DG} \tag{5}$$

In Eq. 5, E_{DG} is the emission of gases from the generator unit (in kg/year), The total amount of fuel consumed by the DG unit is presented by F_{DG}, and the factor of gas released by the generator (kg of gas /per liter of fuel) is represented by EF_{DG}. The Eq. A3 in the appendix section shows the formula for calculating the total emission of gases emitted by the generator.

2.3. Mathematical modelling of grid energy export and import

The major source of energy to meet the demand of the university is the utility network, which is supplied by the Islamabad Electric Supply Company (IESCO). The university relies heavily on grid energy to meet its consumption needs. Although there is a net metering system that allows the university to sell excess energy back into the grid. The total energy consumption can be calculated using the following equation [47].

$$T_{AEC} = \sum_{rates\ r} \sum_{m=1}^{12} \left(E_{buy,r,m}.\ C_{buy,r}\right) - \sum_{rates\ r} \sum_{m=1}^{12} \left(E_{sell,r,m}.\ C_{sell,r}\right) \tag{6}$$

T_{AEC} is the total annual energy charge of electricity. $E_{buy,r,m}$ is the energy purchased (kWh) from the grid at rate r in the month m, and $C_{buy,r}$ is the cost of per unit energy ($/kWh), which is purchased from the grid. $E_{sell,r,m}$ is the energy export to grid (kWh) at rate r during the month m, and $C_{sell,r}$ is the cost per unit energy ($/kWh), which is exported back to the grid. Eq. A4 in the appendix section is used to calculate the annual demand cost from the grid.

Total annual grid cost can be calculated by Eq. A5 in the Appendix section, where $P_{demand,r,m}$ is the power purchased from grid (kW) at rate (r) in month (m) and $C_{demand,r}$ is the demand charge ($/kW). Eq. A7 in the Appendix section calculates total energy cost using peak and off-peak rates. Table 3 indicated various techno-economic parameters of the grid [54].

2.4. Mathematical modelling of solar PV

The energy produced from PV panels depend upon available solar resources. The power generated from PV array is calculated using equation 7 [55,56].

$$P_{PV_{out}}(t) = P_{rated} \times \mu_{der} \times \left(\frac{S_h(t)}{S_{STC}}\right) \times [1 + \beta_{TEMP}(T_{mod} - T_{STC})] \tag{7}$$

In equation 7, the term P_{rated} is the rated power of solar PV array (kW). The term.

"μ_{der}" stands for the derating factor of the PV panels, while " $S_h(t)$" represents the hourly average solar irradiation. "S_{STC}" is the solar irradiation under standard test conditions (STC). "β_{TEMP}" is the temperature coefficient of the PV panels measured in (%/°C), "T_{mod}" represents the module temperature, "T_{STC}" is the temperature of the module under standard temperature conditions in°C, and "P_{rated}" is the rated power of the solar PV panel. At night, the temperature of the PV cell $T_{mod}(t)$ is equal to the ambient air temperature $T_{amb(t)}$.

During the day, the temperature of the PV cell $T_{mod}(t)$ is calculated using the formula given in Eq. 14 [56]. Eq. 8 defines $T_{mod}(t)$ as the module temperature, $T_{amb(t)}$ as the ambient air temperature, and $T_{amb,ref}$ as the ambient temperature under nominal conditions. S_{ref} is the irradiance, and ς_{mp} is the PV system efficiency at maximum power. Ψ and φ are dimensionless solar transmittance and absorptance factors, typically calculated as 0.9. The new equation for the PV cell temperature is derived accordingly. The techno-economic parameters of the solar PV model used in the study are presented in Table A2 in appendix section [55,56].

$$T_{mod}(t) = T_{amb(t)} + (T_{mod,ref} - T_{amb,ref}) \times \left(\frac{S_h(t)}{S_{ref}}\right) \times \left(1 - \frac{\varsigma_{mp}}{0.9}\right) \tag{8}$$

2.5. Mathematical modelling of two-way power converter

To avoid any failure, the converter is designed to meet the maximum load demand $P_{Max\ Load}(t)$. The size of the converter is calculated based on the Eq. 9 [57,58].

$$P_{conv}(t) = \frac{P_{load,\ max}(t)}{\eta_{effi}} \tag{9}$$

In the Eq. 9, η_{effi} represents the efficiency of the converter. Table A2 in appendix presents the detailed techno-economic details of converter [57].

2.6. Mathematical modelling of wind turbine

The wind turbine (WT) has a rated power termed as P_{rated}, which is generated at a particular wind speed termed as v_{nom}. The output power of a wind turbine is $P_{Gen,\ WT}$ as given in the formula in Eq. 10 [57,59,60]. The techno-economic parameters of WT are presented in Table A2 in appendix section.

$$P_{Gen,WT} = \begin{cases} 0 & 0 \le \nu(t) \le v_{start}\ \nu(t) \ge v_{stop} \\ v^3(t)\left(\frac{P_{rated}}{v_{nom}^3 - v_{start}^3}\right) - v_{start}^3\left(\frac{P_{rated}}{v_{rated}^3 - v_{cutin}^3}\right) & v_{start} < \nu(t) < v_{nom} \\ P_{rated} & v_{nom} \le \nu(t) < v_{stop} \end{cases} \tag{10}$$

2.7. Mathematical modelling of battery energy storage system (BESS)

Batteries are used to store extra energy when the RES's output surpasses the needs of the current load. The batteries then provide the stored energy when the generated energy is not enough to meet the demands of the system. The batteries effectively store and provide the system with alternating current (AC) voltage. The battery utilized in this investigation is the Li-Ion model. The Eqs. 11 and 12 describe how the battery charges and discharges [61,62].

$$SOC_{bat}(t) = SOC_{bat}(t-1) \times (1-\tau) + \left(P_{Gen,\ WT} \times \eta_{effi} + P_{PV_{out}}(t) - P_{demand}(t) - \frac{P_{Load}(t)}{\eta_{effi}}\right) \times \eta_{chg} \tag{11}$$

$$SOC_{bat}(t) = SOC_{bat}(t-1) \times (1-\tau) - \frac{\left(\frac{P_{Load}(t)}{\eta_{effi}} - P_{aux}(t) - P_{PV_{out}}(t) - P_{Gen,\ WT}(t) \times \eta_{effi}\right)}{\eta_{dch}} \tag{12}$$

The behavior of the battery is determined by self-discharge τ, charging efficiency η_{chg}, discharging efficiency η_{dch}, and converter efficiency η_{effi}; it depends on the minimum state of charge SOC_{bat}^{min} depth of discharge (DOD_{batt}), and the battery capacity Cp_{batt}, as represented Eq. A8 in appendix section [63]. The techno-economic parameters of the BESS are summarized in Table A2 in the appendix section [64].

2.8. Mathematical modelling of diesel generator

The slope of the generator's fuel curve indicates how much fuel is consumed for each extra unit of power produced. The slope is determined by drawing a line on a graph connecting power output and fuel consumption, which is further used to calculate hourly fuel usage based on electrical output, as given in Eq. 13 [65].

$$P_{DG}(t) = P_{Load}(t) + P_{Losses}(t) \tag{13}$$

In Eq. 13, $P_{DG}(t)$ is the generator's output (kW) at time (t), which supplies the load $P_{Load}(t)$ while also accounting for system losses $P_{Losses}(t)$. Fuel consumption is calculated using equation A9, and costs are calculated using Eq. A10 in the appendix section.

2.9. Mathematical modelling of electrolyzer

An electrolyzer uses electrolysis to separate water into hydrogen and oxygen, powered by electrical energy. Types include PEM, solid oxide, phosphoric acid, direct methanol, and alkaline electrolyzers. PEM electrolyzers, with a practical efficiency of 85% (theoretical max of 94%), are ideal for rural applications. This study assumes an 85% efficiency for the PEM electrolyzer, with the required energy and hydrogen production rate calculated using Eqs. 14 and 15.

$$I_E = A_E.mH_2 + B_E.m'_{H_2} \tag{14}$$

$$Q_{H_2} = n_f\left(\frac{N_c I_e}{2F}\right) \tag{15}$$

2.10. Mathematical modelling hydrogen tank

Hydrogen produced by the electrolyzer is stored in a tank using a compressor, with energy requirements calculated by Eqs. 16. Eq. A11 (appendix) calculates the pressure of the hydrogen tank, while Eq. A12 (appendix) estimates hydrogen production from electrical energy using the lower heating value of hydrogen [66].

$$P_{comp} = R\left(\frac{T_{htci}}{\mu_{htc}}\right) Q_{H_2}\left(\frac{\gamma}{\gamma-1}\right)\left[\left(\frac{P_{hto}}{P_{hti}}\right)^{\left(\frac{\gamma}{\gamma-1}\right)} - 1\right] \tag{16}$$

2.11. Mathematical modelling fuel cell

This research uses PEM fuel cells, which are ideal for autonomous power systems due to their high efficiency, long lifespan, lightweight design, low temperature, low maintenance, quiet operation, high capacity, and low emissions. The performance and power of the fuel cell were calculated using Eqs. 17 and 18 [66]. The PEM electrolyzer was modeled in HOMER Pro using a capital cost of \$1,100/kW, a replacement cost of \$850/kW, and fixed annual O&M of \$10/yr. The nominal electrolyzer efficiency was set to 85%.

$$\eta_{FC} = \frac{P_{FC}}{m_{H_2} HHV_{H_2}} \tag{17}$$

$$P_{FC} = V_{stack} I_{FC} = V_{SC} N_{cell} I_{FC} \tag{18}$$

3. Results of study

This study assesses the ability of HRES to ensure that they can adequately meet the load demand. The effectiveness of renewable energy projects depends on their technical and economic feasibility. While economic opportunities attract investors and offer affordable prices, technical feasibility ensures a stable energy supply. Energy production profiles are analysed throughout the year to verify the robustness of the system.

3.1. Techno-economic results

An initial assessment is necessary to ensure that the proposed energy system efficiently meets energy needs. Many energy projects in developing countries fail due to an insufficient understanding of load demand. This study examines the available energy resources, the socioeconomic environment, and the load demand of the selected area, which helps in the accurate modelling of HRES. Techno-economic analysis optimizes system component sizing without compromising energy cost and reliability. HOMER generated multiple scenarios, and only those feasible in terms of cost, net present cost, and reliability were selected.

3.1.1. Scenario I: base case: grid and diesel generator

The base case consists of a utility grid and a DG. DG is used as a backup energy source during load shedding or any other contingency situation. In the base case, the entire energy is imported from the grid, which is 5,005,975 kWh/yr. There is no excess energy available in this system, and there are no capacity shortages as well. Two cases are considered in this scenario: one with DG and the other without DG. The LCOE is different for both cases. The LCOE for the system of grid-only system is $0.0856/kWh with an NPC of $9.51M, while the LCOE of the system containing DG is $0.0838/kWh with an NPC of $9.32M. The LCOE of the system containing DG is lower compared to other systems due to the salvage cost that is obtained from the DG. The other costs associated with the base scenario are presented in Table A7 in the appendix section.

3.1.2. Scenario II: solar PV with BESS

The second scenario obtained from optimization contains Solar PV and BESS. This system is a 100% renewable energy-based system consisting of 25000 KW of solar panels, 11,728 kWh of Li-Ion BESS, and a converter size of 1404 kW. Solar farm produces a total of 38,997,768 kWh/yr of energy, fulfilling the load demand of 5,003,586 kWh/yr. Since this system is isolated from the grid, the BESS fulfils the load demand when the solar energy is not available.

The batteries remain fully charged during the daytime when there is an availability of solar energy and are utilized from evening and during the whole night from 6 PM to 6 AM. The LCOE for this system is $0.2008/kWh with an upfront cost of $22.3M, as shown in Fig. 5. The capital cost of PV panels is $6,475,000 with an O&M cost of $1,870,539.50. The capital cost of BESS is $2,345,600 with an O&M cost of $2,603,879, and a replacement cost of $8,363,754.03. The costs associated with this Scenario are presented in Table A8 in the appendix section. The major driver of higher LCOE in this system is BESS, since the lifetime of BESS is 5 years, and they need to be replaced after 5 years, which drives the cost of energy higher in this system.

3.1.3. Scenario III: solar PV, grid with BESS

In the third scenario, along with Solar PV and BESS, the grid is also integrated. This system is also 100% renewable energy-based system consisting of 25000 kW of solar panels, 28,128 kWh of Li-Ion BESS, and a converter size of 1353 kW. Solar farm produces a total of 38,997,768 kWh/yr of energy, fulfilling the load demand of 5,003,586 kWh/yr. Since this system is grid-connected, the excess amount of energy is sold back to the grid.

The total amount of energy sold back to the grid is 2,724,533 kWh/yr, and nothing is imported from the grid. During the daytime, when solar energy is available in excess, the excess energy is sold back to the grid. Batteries are also charged during the daytime during excess availability of solar energy, which are discharged at night from midnight to 6 AM. The total amount of energy in for BESS is 3,841,119 kWh/yr, and the value of energy out is 3,465,912 kWh/yr, with total losses of 384,594 kWh/yr. A total of 3516 strings in parallel are connected, with each string containing 8 batteries.

The LCOE for this system is $0.215 with an NPC of around $37M as

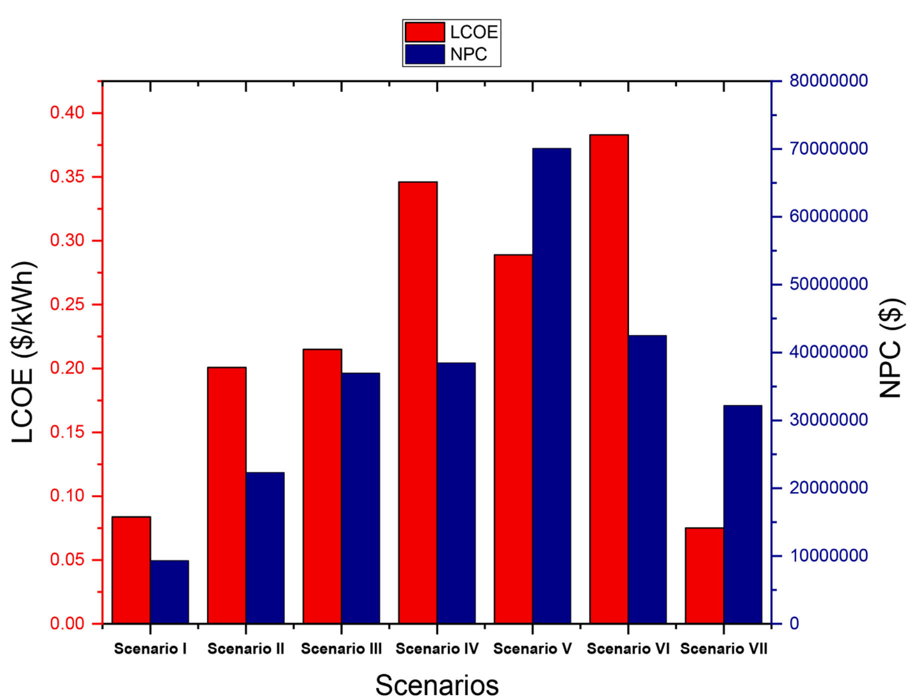

Fig. 5. LCOE & NPC of different hybrid energy systems scenarios (I-VII).

presented in Fig. 5. Table A9 in the appendix section shows the different types of costs associated with this system. The capital cost of PV panels is $6,475,000.00 with an O&M cost of $1,870,539.50. The capital cost of BESS is $6,475,000.00 with an O&M cost of $6,245,048.68, and a replacement cost of $20,059,317.31. The capital cost of the system converter is $202,950.00, the O&M cost of is $300,396.43, and the replacement cost is $176,518.16.

3.1.4. Scenario IV: solar PV, wind with BESS

The optimization results of this Solar PV, Wind, and BESS system include 15 MW solar PV, 726 WTs (each turbine has a capacity of 10 kW), 1418 kW power converter, 16 kWh Li-Ion BESS (string size 8 with 2000 strings in parallel). The system provides a total amount of 25,384,496 kWh/yr of energy, out of which 23,398,661 kWh/yr of energy (92.2%) is generated from PV panels, while 1,985,835 kWh/yr (7.82%) is produced from WTs. This system is also 100% renewable energy-based system.

The capacity factor for PV panels is 17.8% with an LCOE of 0.00964 $/kWh. The capacity factor for WTs is 3.12% with an LCOE of 0.332 $/kWh. The Energy in of the BESS is 2,021,085 kWh/yr, and Energy out is 1,824,512 kWh/yr with total losses of 202,408 kWh/yr. Similar to previous systems in scenarios II and III, in this scenario, the BESS are charged during the excess availability of solar energy and discharged when solar energy is not available from 8 PM to 6 AM.

The capital cost for wind turbines is $10,890,000 with a replacement cost of $7,534,372, and an O&M cost of $1,611,883. The BESS costs $3,200,000 in terms of capital cost, $11,410,305 as in replacement cost, and $3,552,359.88 in O&M expenses. The PV system has a capital cost of $3,885,000 with a replacement cost of $1,122,323. The power converter incurs a capital cost of $212,639, a replacement cost of $184,945, and an O&M cost for the power converter of $314,738. Table A10 in the appendix section represents different costs associated with Scenario IV. The overall LCOE for this system is $0.346 with an NPC of $38.5M as shown in Fig. 5.

3.1.5. Scenario V: solar PV, wind, and grid with BESS

Scenario V consists of Solar PV, Wind, BESS, and Grid. This system is also 100% renewable energy-based system consisting of 15 MW of solar panels, 32,000 kWh of Li-Ion BESS, 1798 WTs (each turbine is 10 kW), and a converter size of 1305 kW. PV panels produce a total of 23,398,661 kWh/yr of energy with an 82.2% of contribution to the energy mix, and rest of 17.4% is generated from wind turbines.

Though this system is grid-connected, energy is not imported from the grid; however, some energy is sold back to the grid after fulfilling the load demand of 5,003,586 kWh/yr. The total amount of energy sold back to the grid is 5,901,295 kWh/yr, and nothing is imported from the grid. During the daytime, when solar energy is available in excess, the excess energy is sold back to the grid. Batteries are also charged during the daytime, during excess availability of solar energy, which are discharged at night from midnight till 6 AM. The total amount of Energy in for BESS is 3,630,092 kWh/yr, and the value of Energy out is 3,275,808 kWh/yr with total losses of 363,481 kWh/yr.

A total of 4,000 strings in parallel are connected, with each string containing 8 batteries. The capacity factor for PV panels is 17.8% with an LCOE of 0.00964 $/kWh. The capacity factor for WTs is 3.12% with an LCOE of 0.332 $/kWh. The capital cost of PV panels is $3,885,000.00 with an O&M cost of $1,122,323.70. The capital cost of BESS is $6,400,000.00 with an O&M cost of $7,104,719.77, and a replacement cost of $22,820,611.27. The capital cost of the system converter is $195,752.40, the O&M cost is $289,742.90, and the replacement cost is $170,257.96. WTs have a capital cost of $26,970,000.00, a replacement cost of $18,659,506.1, and an O&M cost of $3,991,964.42. The costs associated with this scenario are shown in Table A11 in the appendix section. The overall LCOE for this system is $0.289 with an upfront cost of around $70.1M, as depicted in Fig. 5.

3.1.6. Scenario VI: solar PV, fuel cell, BESS, electrolyzer, and hydrogen tank

The optimization results of Scenario VI include 28 MW Solar PV, 2100 KW FC, 4000 kWh Li-Ion BESS, 8000 kW electrolyzer, 15000 kg of HT, and 1311 kW power converter. Considering simulation results, the optimized Solar PV, Fuel Cell, BESS, Electrolyzer, and HT, this HRES provides 44,959,939 kWh/yr of total electrical energy with a 100% RF. The solar PV generates 43,677,500 kWh/yr of energy, a mean energy output of 119,664 kWh/d, a capacity factor of 17.8%, and a levelized cost of solar PV is 0.00964 $/kWh.

The FC operates frequently, approximately 2,162 h/yr with 1,282,440 kWh/yr of electrical production. The capacity factor of FC is 6.97 %, and it operates along with BESS when solar energy is not available. The yearly optimized hydrogen production by electrolyzer is 371,626 kg/yr, and the overall LCOH is $5.15/kg. The hydrogen production from the electrolyzer is shown in Fig. 6. The amount of hydrogen at the beginning of the year is 4500 kg, which is 30% relative to the total size of the tank, while at the end of the year, the amount of hydrogen that remains in the tank is 6296 kg, which is 42% relative to the total tank size.

Fig. 5 shows the hydrogen tank level in the first week of January. The capacity of the energy storage system is 8 in one string and 500 strings in parallel. The energy storage system has a capacity of 1,385,767 kWh/yr (energy in) and 1,249,874 kWh/yr (energy out) with a lifetime throughput of 6,587,415 kWh. The yearly energy losses of the storage system stand at 138,722 kWh/yr. Fig. 5 demonstrates the NPC and LCOE of this scenario. The optimized hybrid system has an operating cost of 551,620 $/yr, total NPC of $42.5 million, and LCOE of 0.383 $/kWh. Table A12 in the appendix section contains different costs of components associated with this Scenario.

3.1.7. Scenario VII: grid-solar PV, fuel cell, BESS, electrolyzer, and hydrogen tank

The optimization results of Scenario VII include 30,000 KW, Solar PV, 2100 KW FC, 4000 kWh of BESS, 11,898 kW power converter, 8000 KW electrolyzer, and 10,000 kg HT. Considering simulation results, Scenario VII generates 50,838,592 kWh/yr of total electrical energy with an RF of 90.6%. The solar PV generates 46,797,321 kWh/yr of energy with a mean energy output of 128,212 kWh/d, a capacity factor of 17.8%, and the LCOE of solar PV is 0.00964 $/kWh. The FC operates frequently, approximately 1,144 hrs/yr, with 2,234,570 kWh/yr of electrical production and a capacity factor of 12.1 %.

The monthly optimized hydrogen production by electrolyzer is 560,078 kg/yr, and the overall LCOH is $2.59/kg with 3,000 kg of hydrogen inside the tank at the beginning of the year, compared to its 10,000 kg of storage capacity. Fig. 6 illustrates the hydrogen production from the electrolyzer. Almost all of the hydrogen is consumed, and only 213 kg of hydrogen is left at the end of the year, which is only 2.13% compared to the overall hydrogen storage capacity of the tank. Fig. 7 shows the HT level in the first week of January. The capacity of the energy storage system is 8 in one string and 500 strings in parallel.

The energy storage system has a capacity of 217,635 kWh/yr (energy in) and 195,872 kWh/yr (energy out) with a lifetime throughput of 1,032,335 kWh. The storage system's annual energy losses are 21,764 kWh. Since this system is connected to the grid, the annual amount of energy purchased from the grid is 1,806,700 kWh, while the energy exported back to the grid is 14,293,184 kWh. Energy is sold back to the grid during the daytime when solar energy is abundantly available, while it is imported from the grid between 6 PM to 6 AM, along with energy from BESS and FC. In the overall energy mix, PV panels contribute 92.1%, FC contributes 4.40%, and 3.55% of energy is imported from the grid. The capital cost of BESS is $800,000 with an O&M cost of $888,089.97, and a replacement cost of $2,852,576.41.

The capital cost of the system converter is $1,784,691.56, the O&M cost is $2,641,611.13, and the replacement cost is $1,552,256.56. PV panels incur a capital cost of $7,770,000.00, and O&M cost of

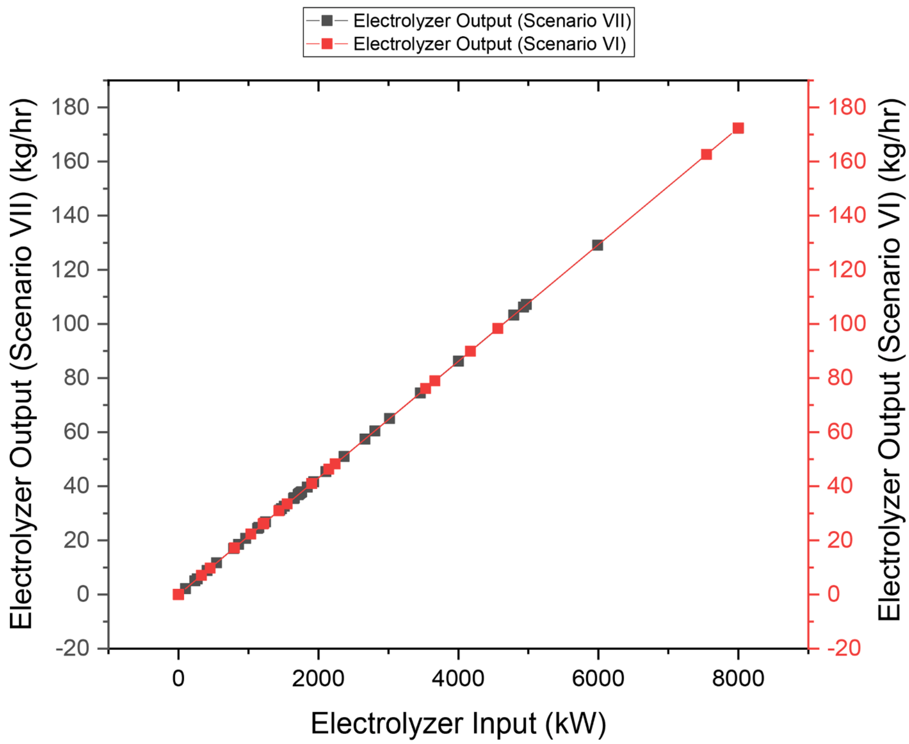

Fig. 6. Hydrogen generation from electrolyzer in scenario VI & scenario VII.

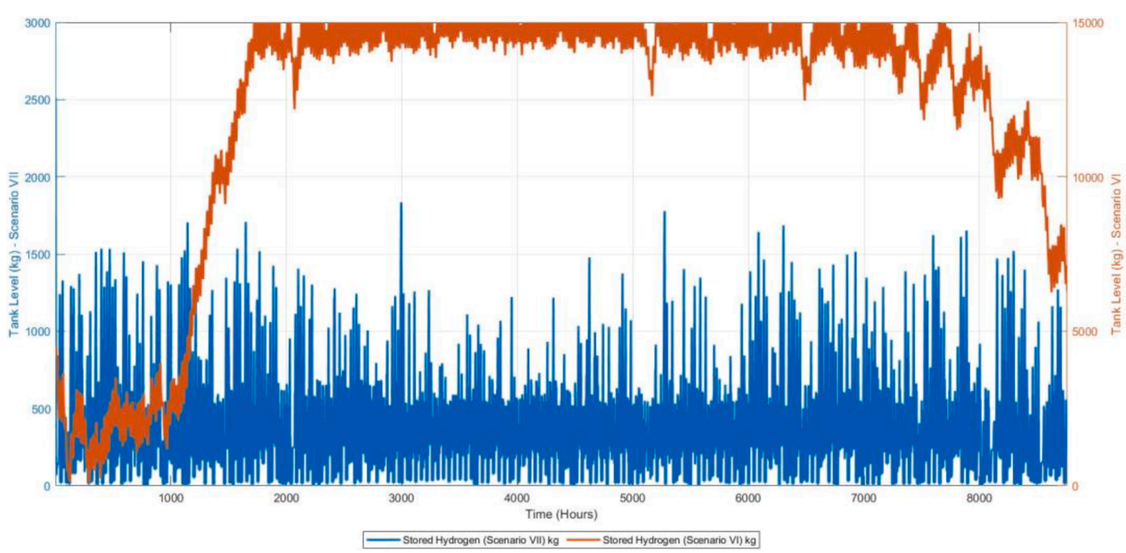

Fig. 7. Hydrogen tank levels in scenarios VI & VII.

$2,244,647.40. The capital cost of FC is $4,200,000.00 with an O&M cost of $1,600,160.51. Fig. 5 demonstrates the NPC and LCOE for Scenario VII. The optimized hybrid system has an operating cost of 127,332 $/yr, a total NPC of $32,181,749.41, and an LCOE of 0.07511 $/kWh. Table A13 in the appendix section presents a breakdown of the costs associated with each component in this scenario.

3.2. *Environmental analysis*

HOMER is used to assess the environmental performance of energy systems. In many cases, DG is combined with renewable energy sources to ensure a continuous supply of electricity throughout the year. HOMER has a preset emission for different components involved in the

Table 2
Emission of pollutants from various energy sources.

Emissions	Grid (g/kWh)	Fuel Cell (g/kg of fuel)	DG (g/kg of fuel)
Carbon Dioxide	632.00	0	13.9
Carbon Monoxide	0.00	–	0.75
Unburned Hydrocarbons	0.00	–	–
Particulate Matter	0.00	–	0.12
Sulphur Dioxide	2.74	–	–
Nitrogen Oxides	1.34	0	2.66

system. Then, the reduction of greenhouse gas emissions is estimated by comparing all the scenarios. Table 2 shows the emission of different gases from various components of HRES. The emissions assessment in this study considers operational CO_2 emissions associated with grid electricity consumption as modelled in HOMER Pro. Lifecycle emissions from manufacturing, transportation, installation, and end-of-life treatment of PV panels, batteries, electrolyzers, and hydrogen storage systems are not included. Therefore, the reported zero-emission scenarios refer to operational emissions only and do not imply full lifecycle carbon neutrality. A constant grid emission factor of 632 g CO_2/kWh was applied as a representative annual average. Time-dependent variations in marginal grid emission intensity were not modelled, which may affect the precision of avoided-emission estimates.

In environmental analysis, the emission of pollutants across all scenarios is considered over the project lifetime. Since some hybrid systems also contain DG, therefore, emissions of carbon dioxide (CO_2), carbon monoxide (CO), unburned hydrocarbons (UH), particulate matter (PM), Sulphur oxide (SOx), and nitrogen oxide (NOx) are taken into account for each system and presented in Table 2. Scenarios II, III, IV, and V are 100% renewable energy-based scenarios; hence, there is no emission from them.100% renewable scenarios eliminate operational grid-related CO_2 emissions under the defined modelling boundary. Scenario I contains DG as a backup source; however, energy is imported from the grid, this system has the highest emission of CO_2, Scenario VI also does not emit any CO_2, which depicts an environmentally friendly Scenario, while Scenario VII emits lesser CO_2 compared to Scenario I due to inclusion of FC and Solar PV, lesser amount of energy is imported from the grid. Compared to the base case, Scenario VII (Optimal Solution) is a better alternative, as during frequent grid outages, this system has very low emissions at a reasonable LCOE. Table 3 provides the emission details of different gases among all scenarios.

The emission reduction of hydrogen systems varies significantly due to regional energy resources and technical configurations in different climate zones. In arid areas where the potential for solar energy is high, such systems can achieve significant emission reductions, mainly because of the abundance of renewable energy. On the other hand, in temperate regions that continuously rely on wind and solar energy, a smaller decrease is often observed, as the need for additional storage or backup systems increases emissions. In warm regions that harness both solar and wind energy, significant reductions can even be achieved, although infrastructure and maintenance costs may be higher.

Furthermore, the reductions also depend on the size of the system that is designed, as depicted by the Fig. 8, which clearly shows that the designed system has significantly reduced the carbon emission compared to systems across the globe. The Emissions reductions also depend on the size of the hydrogen system, particularly the electrolyzers, storage facilities, and fuel cells. Large electrolyzers are more efficient and cost-effective, leading to greater savings. Large storage systems enable better integration of renewable energies, reducing dependence on fossil fuels. Smaller systems may face efficiency challenges, limiting their ability to reduce costs.

3.3. Social parameters analysis

When renewable energy parameters are installed, people from different backgrounds are employed throughout the whole lifetime of the project, from its construction to operation till its decommissioning. Therefore, in this article, a social aspect assessment criterion is considered to quantify the number of jobs created during the projects. Table 4 provides information on the employment potential of different scenarios [66].

This study examines the relationship between employment opportunities and their social impacts. According to the study, the creation of employment opportunities has a positive and significant effect on local communities and individuals. The results particularly show that employment opportunities increase income and financial stability, which improves quality of life and reduces poverty. Table 5 highlights the significant impact of social aspects on community well-being, provides a comprehensive summary of the social assessment for all proposed systems, and clarifies the social outcomes.

3.4. Robustness analysis

This study evaluated the reliability of HRES, which determines whether it is suitable or not to meet the demand in the proposed region. Techno-economic feasibility plays a key role in the successful implementation of energy projects. The energy system must be economically viable for initial users and investors interested in investing in energy projects. At the same time, it is also essential to ensure a reliable and safe electricity supply. Therefore, robustness is analysed and verified through energy generation profiles.

The robustness analysis for all scenarios has been carried out based on three main parameters: (a) Excess energy in the system, (b) Unmet load, and (c) Capacity Shortage. Table 6 presents the robustness analysis of all energy scenarios, evaluating additional energy in the system, Unmet load, and capacity deficiency under different configurations. Each scenario represents the balance between energy supply and demand, and shows how well each configuration performs in terms of energy reliability, cost-effectiveness, and the ability to handle load fluctuations. The objective is to determine which scenario provides sufficient energy for emergencies while minimizing unnecessary costs associated with additional generation.

Scenario I functions as a baseline, where there is no additional energy, unsatisfied demand, or insufficient capacity. Although in practice, this is almost unattainable, this ideal condition reflects a system that is fully balanced. It describes a situation in which the energy supply always matches the demand, leaving no room for unexpected loads or system failures. Scenario II shows the highest amount of additional energy (33,197,099 kWh/year, or 85.1%), along with a lack of capacity and inaccessible demand. The additional energy allows the system to handle any change, but it also indicates overproduction, which could increase costs without benefit. While this ensures reliability, excessive additional energy may not be economically suitable for most applications, as the system's production is much higher than necessary, resulting in inefficiencies.

In Scenario III, there is no unmet load, but the additional energy is slightly lower (30,033,108 kWh/year or 77.0%). Although the system generally operates efficiently, there are small-scale performance risks during peak high-demand periods, as indicated by its slight capacity shortfall (0.0012%). While this scenario is more balanced compared to

Table 3
Emission of gases in different scenarios.

Emission Species (kg/yr)	Scenario I	Scenario II	Scenario III	Scenario IV	Scenario V	Scenario VI	Scenario VII
Carbon Dioxide	3,163,776	0	0	0	0	0	1,127,240
Carbon Monoxide	0	0	0	0	0	6,102	9,287
Unburned Hydrocarbons	0	0	0	0	0	266	405
Particulate Matter	0	0	0	0	0	37.0	56.3
Sulphur Dioxide	13,716	0	0	0	0	0	4,950
Nitrogen Oxides	6,708	0	0	0	0	5,732	11,145

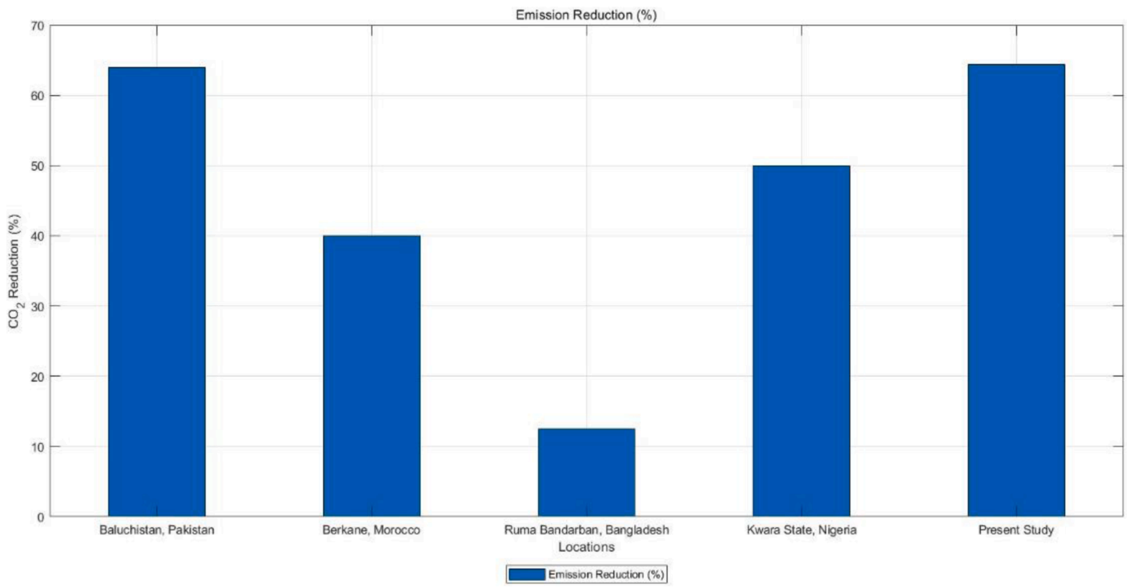

Fig. 8. Comparison of emission reduction of present study with different locations in World in Baluchistan Pakistan [82], Berkane Morocco [83], Ruma Bandarban Bangladesh [84], Kwara Sata Nigeria [85].

Table 4
Employment potential of different energy sources.

Sr. No.	Energy Supply System	Jobs Created (10^{-7} jobs/kWh/year)	Jobs creation (jobs/TWh/year)
1	Solar Energy	0.27549	28
2	Wind Energy	0.27549	28
3	Fuel Cell System	0.27549	28
4	Genset	0.27549	28

Scenario II, it may require further improvements to ensure full coverage during infrequent demand peaks. In Scenario IV, there is a small, incomplete load and a capacity shortfall of 0.0989%, but the additional energy is minimal, 19,761,553 kWh/year (77.8%). This scenario provides room for unforeseen conditions and provides a sufficient amount of additional energy to cover normal fluctuations. The system can still meet maximum demand, as the available additional energy is adequate, even reducing the risk of overproduction.

For applications that want to be reliable without unnecessary energy waste, this is a complete and effective option. In Scenario V, the decrease in capacity is minimal, just 0.003%, but it stands out with 16,284,942 kilowatt-hours/year (57.5%) of additional energy and no unmet demand. In this more conservative scenario, cost efficiency is prioritized by reducing the production of additional energy. While this strategy lowers costs, it also makes it more difficult to manage large variations in system demand, increasing the likelihood of capacity shortfalls during extraordinary demand peaks.

In Scenario VI, there is a small capacity shortfall of 0.003%, but it shines with 22,018,841 kWh/year (49%) of additional energy, and there is no unmet demand. In this more conservative scenario, cost efficiency is prioritized by reducing the production of additional energy. Although this strategy reduces costs, it also makes it difficult to manage large fluctuations in system demand, thereby increasing the likelihood of a capacity shortfall during periods of exceptionally high demand.

In Scenario VII, there is a small unmet load, with a slight decrease in capacity (0.0382%), and the minimum amount of additional energy is 35,552.16 kWh/year (6.99%). Although the capacity to store additional energy in this scenario is quite limited, it is still sufficient to cover normal demand fluctuations. It is a very economical solution, as the amount of additional energy is low, which reduces costs related to additional production. However, if faced with particularly high demand, the additional 6.99% reserve may not be enough during a sudden spike in demand, which could cause capacity shortages.

Scenario VII is the most coherent and precise option in terms of

Table 6
Robustness analysis of different scenarios.

Scenarios	Parameters					
	Excess energy		Unmet Load		Capacity Shortage	
	(kWh/Yr)	%	(kWh/Yr)	%	(kWh/Yr)	%
Scenario I	0	0	0	0	0	0
Scenario II	33,197,099	85.1	2,389	0.0477	4,881	0.0975
Scenario III	30,033,108	77.0	0	0	61.6	0.00120
Scenario IV	19,761,553	77.8	3,535	0.0706	4,951	0.0989
Scenario V	16,284,942	57.5	0	0	152	0.00300
Scenario VI	22,018,841	49.0	2,157	0.0431	4,106	0.0820
Scenario VII	3,555,216	6.99	1,556	0.0311	1,912	0.0382

Table 5
Job creation in different scenarios.

Jobs Creation/Yr	Scenario I	Scenario II	Scenario III	Scenario IV		Scenario V		Scenario VI		Scenario VII	
	No Job is created	1.074 jobs/year	1.074 Jobs/Year	Solar PV creates 0.644 jobs/Year	Wind Energy creates 0.0547 jobs/Year	Solar PV creates 0.645 jobs/Year	Wind Energy creates 0.135 jobs/Year	Solar PV creates 1.203 jobs/Year	Fuel Cell creates 0.035 jobs/Year	Solar PV creates 1.289 jobs/Year	Fuel Cell creates 0.062 jobs/Year

reliability, especially in a university setting. It offers an effective balance between reliability and cost savings, in addition to providing an extra 7% of energy. This additional amount of energy is sufficient to manage normal load changes in a university environment without generating unnecessary excess production, which could lead to additional expenses. Scenario VII minimizes unmet loads and lack of capacity through the integrated operation of the grid, BESS, and FCs. Grid connection plays a key role in absorbing the remaining demands, especially during long periods in the afternoon and evening when photovoltaic production is zero, and stored hydrogen levels are low.

BESS reduces short-term fluctuations and peaks and ensures that the short-term imbalance between PV production and demand is balanced without resorting to imports from the grid. For long-term bottlenecks, particularly during multi-hour periods of low sunlight, the fuel cell powered by hydrogen generated through electrolysis from excess PV production offers an attractive backup power supply. This multi-layered approach allows view VII to maintain a high level of reliability, even though it has the smallest margin for surplus energy among all views (6.99%). The grid serves as a last safety net for rare and highly demanded situations, while hydrogen and battery storage control most of the internal variables. As a result, the capacity shortfall is limited to 0.0382%, and unmet demand remains low, so small that practical disruptions can be avoided in a university setting. This synchronization between multiple supply sources ensures a repair without the need for excessive expansion of the generation or storage systems. In fiscal year (FY) 2022–23, the reliability performance of IESCO indicates substantial deviation from regulatory benchmarks. Under Rule 4(b) of the Performance Standards (Distribution) Rules 2005 [67], the System Average Interruption Duration Index (SAIDI) must not exceed 14 min annually; however, IESCO reported a SAIDI value of 1,006.34 min, reflecting prolonged outage durations experienced by consumers during the year. Additionally, IESCO recorded a fault rate of 4.63 faults per kilometer, indicating frequent infrastructure-related disturbances within the distribution network. These figures demonstrate that despite comparatively better performance than several other DISCOs, the conventional grid supply under IESCO remains prone to interruptions and reliability limitations [68]. In contrast, Scenario VII of the proposed hybrid system exhibits a capacity shortage of only 0.0382% and an unmet load of 0.0311%, signifying a substantially higher level of supply continuity and system robustness. The comparison clearly shows that the hybrid

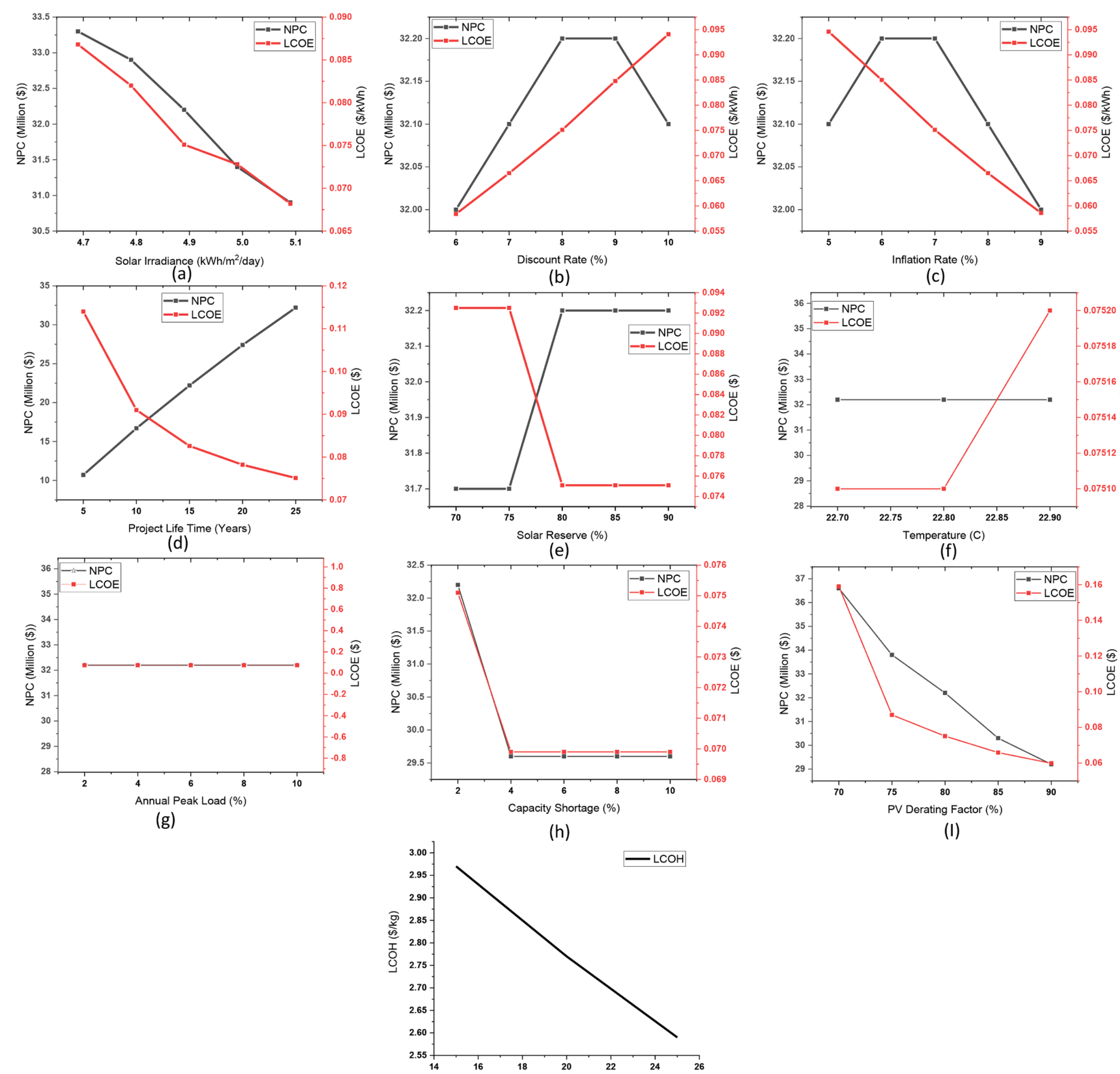

Fig. 9. Impact of different sensitivity parameters on LCOE & NPC (a) Solar Irradiance (b) Discount Rate (c) Inflation Rate (d) Project Lifetime (e) Solar Reserve (f) Temperature (g) Annual Peak Load (h) Capacity Shortage (I) PV Derating Factor (J) LCOH with Electrolyzers Lifetime.

configuration provides enhanced reliability by minimizing outage risk and reducing dependence on grid-induced interruptions, thereby offering a more resilient energy solution for the campus.

3.5. Sensitivity analysis

Sensitivity analysis examines how key parameters affect the NPC and the LCOE in hybrid renewable energy systems. Based on the energy sector of Pakistan and economic conditions, key variables include the nominal discount rate, inflation rate, project lifetime, solar radiation, load demand, etc. Of these, the inflation rate has the greatest impact because its consistently high prices significantly affect the cost of imports. Understanding the impact of these variables helps to interpret the results from the investor's perspective, supporting more informed decisions in the context of renewable energy development. The effects of these sensitivity parameters are observed on Scenario VII (Grid-Solar PV, FC, BESS, Electrolyzer, and HT), which is considered the most optimal scenario among all others.

Solar irradiance is varied by (± 1) in the reference value of 4.89 kwh/m^2/day to observe the effects of variation on NPC and LCOE for the optimal scenario (Scenario VII). Fig. 9 (a) explains that as solar irradiance increases the NPC and LCOE dwindle down. The value of NPC and LCOE decrease from $33.2 M to around $30.7M and LCOE decreases from 0.0868 $/kWh to $0.0682 as the value of irradiance increases from 4.69 to 5.09 kwh/m^2/day. NPC and LCOE decrease as the value of irradiance increases from reference value and decreases as the solar irradiance decreases down.

Fig. 9 (b) shows the variation in NPC and LCOE as the discount rate varies from reference value of 8%. NPC of the optimal scenario is lower at the lower discount rates and as the discount rate increases, however, the LCOE increases with the increase in discount rate as evident from the figure. The LCOE increases from 0.0751 $/kWh to 0.0941 $/kWh with increase in discount rate from reference value to 10% and decreases to 0.0584 $/kWh as the discount rate decreases to 6% from reference value. NPC decreases from $32.2 M to $32M as the discount rate hits at 6% and is $32.1M at 10% discount rate.

Fig. 9 (c) shows the impact of variation in inflation rates from its reference value of 7% on NPC and LCOE. As the inflation rate decreases from reference value to 6% there is no impact on NPC, however, as the inflation goes to 5%, the NPC decreases to $32.1 M. However, the LCOE drastically reduces from 0.0751 (LCOE at reference value) to 0.0586 $/kWh and increases to 0.0946 $/kWh as the inflation rate lessens to 5% from 7%.

Fig. 9 (d) elucidates how change in project life time impacts NPC and LCOE for the optimal Scenario. LCOE increases with the decrease in project life time, however, NPC increases with the increase in project life time. LCOE increases from 0.0751 $/kWh (at reference life time of 25 years) to 0.114 $/kWh (at project life time of 5 years). On the other hand, the NPC decreases from $32.2 M (at reference life time of 25 years) to $10.7M (at the project life of 5 years).

Fig. 9 (e) shows the variations in solar reserve and its impacts on NPC and LCOE on scenario VII. Solar reserve is varied by 5% from 80% to 70% and 90% to observe the impacts of both increment and decrement. When the solar reserve decreases from its reference value (80%), the LCOE increases to 0.0951 $/kWh from 0.0751 $/kWh and NPC also decreases from $32.2 M to $31.7 M at 70% of solar reserve.

The temperature is varied by (± 0.05 C) from reference value of around 22.80. Fig. 9 (f) depicts the impact of temperature on NPC and LCOE. The increase in temperature does not affect the NPC at all and it remains constant $32.2M, however, as the temperature increases to 22.90 C, the LCOE increases 0.0752 $/kWh.

Fig. 9 (g) shows the impacts of variation of annual peak load on NPC and LCOE. There is no effect of changes in annual peak load on both LCOE or NPC due to access energy available in the system, these variations can be easily manipulated. Fig. 9 (h) shows the changes in capacity shortage and its impacts on both LCOE and NPC of the system. It is evident that as the capacity shortage increases both NPC and LCOE reduce. The NPC decreases from $32.2M to $29.6M and LCOE also decreases from $0.0751 to $0.0699.

Fig. 9 (I) elucidates the impacts of derating factor of solar panels. As the derating factor decreases from its reference value of (80%) to 70%, NPC increases to $36.6M from $32.2M and LCOE increases to 0.159 $/kWh from 0.0751 $/kWh. However, as derating factor increases to 90% from 80%, the NPC decreases to $29.2M from 32.2M and LCOE decreases to 0.0599 $/kWh from 0.0751 $/kWh.

To address uncertainty in stack life and replacement timing, a sensitivity check is also performed by reducing the electrolyzer lifetime to 20 years and 15 years, as depicted in Fig. 9 (J). The resulting LCOH values exhibited only a modest change across Scenario VII, indicating that under the optimized operating strategy (high PV-driven utilization and use of excess generation), the LCOH remains relatively stable with respect to reasonable lifetime variations. This provides additional confidence that the reported LCOH is not solely dependent on an optimistic lifetime assumption.

4. Discussion and policy implications

This section describes the optimization strategies adopted for different scenarios and explains their impacts on sustainability, profitability, renewable energy integration, and hydrogen production capacity. It also presents a comparative analysis of various systematic scenarios, with a particular focus on Scenario VII, considered the best HRES and the most sensitive in terms of solar resource availability, technical performance, and economic conditions. This section also evaluates the role of hydrogen integration in Scenarios VI and VII, and estimates the impacts on the campus's energy sustainability, infrastructure needs, and practical implementation.

Additionally, this scenario presents a detailed analysis of the economic performance of Scenario VII, including its NPC, LCOE, and LCOH, and compares these results with global standards and future cost targets. Finally, the discussion highlights the broad economic and practical impacts of implementing such systems, emphasizing the competitiveness of green hydrogen under favourable conditions and the practical challenges required to replicate the model's performance in the real world. Two types of strategies were employed in the optimization process: LF and CC.

To remain reliable during extended periods with limited resources, LF prioritizes meeting the demand for PV energy and FCs while keeping storage at a minimum level. This approach can direct additional solar production toward low-cost hydrogen generation and generally reduces grid energy purchases and operating costs. In contrast, CC charges the battery whenever additional solar energy is available (and grid energy if necessary), keeping it in a state of overcharge. This increases autonomy, reduces the risk of incomplete charges, decreases battery cycle depth and stress from transitions, and maintains fuel cell readiness. Therefore, the choice between LF and CC requires a balance between reliable outcomes, cost-effectiveness, renewable energy integration, and hydrogen generation capacity. The inclusion of a comprehensive campus load profile, incorporating both academic facilities and residential hostels, represents a critical modelling strength of this study. Unlike academic-only loads, which are predominantly daytime-oriented and closely aligned with solar PV generation patterns, the mixed-load profile introduces significant evening and night-time demand due to hostel consumption. This temporal mismatch between renewable generation and demand increases the need for both short-term (BESS) and long-term (hydrogen) storage solutions. If only academic loads were considered, the system would demonstrate improved solar-load alignment, reduced storage requirements, and potentially lower hydrogen utilization. However, such a simplification would underestimate real storage needs and overestimate renewable integration performance. By incorporating hostel loads, the model captures realistic campus energy behavior, thereby providing a more robust assessment of storage sizing, hydrogen production capacity, and long-term reliability.

The overall results show that in scenarios VI and VII, hydrogen integration plays an important role in improving long-term energy reliability, as it provides seasonal storage capacity and supports continuous supply during extended periods of low renewable generation. Based on the simulation results, scenario VII, with a lower NPC ($32.18 million) and LCOE ($0.0751/kWh), offers clear practical benefits. This system integrates PV, BESS, hydrogen storage, fuel cells, and grid connectivity, resulting in a multidimensional energy supply strategy. During grid outages or extended periods of low solar radiation, the BESS provides immediate short-term backup power, while the fuel cell, powered by on-site generated hydrogen, ensures a continuous energy supply. This capability increases reliability compared to other scenarios that rely only on short-term BESS or intermittent renewable energy.

The great strength of Scenario VII lies in its hydrogen fusion. An 8 MW electrolyzer produces 560,078 kgs of hydrogen annually from the

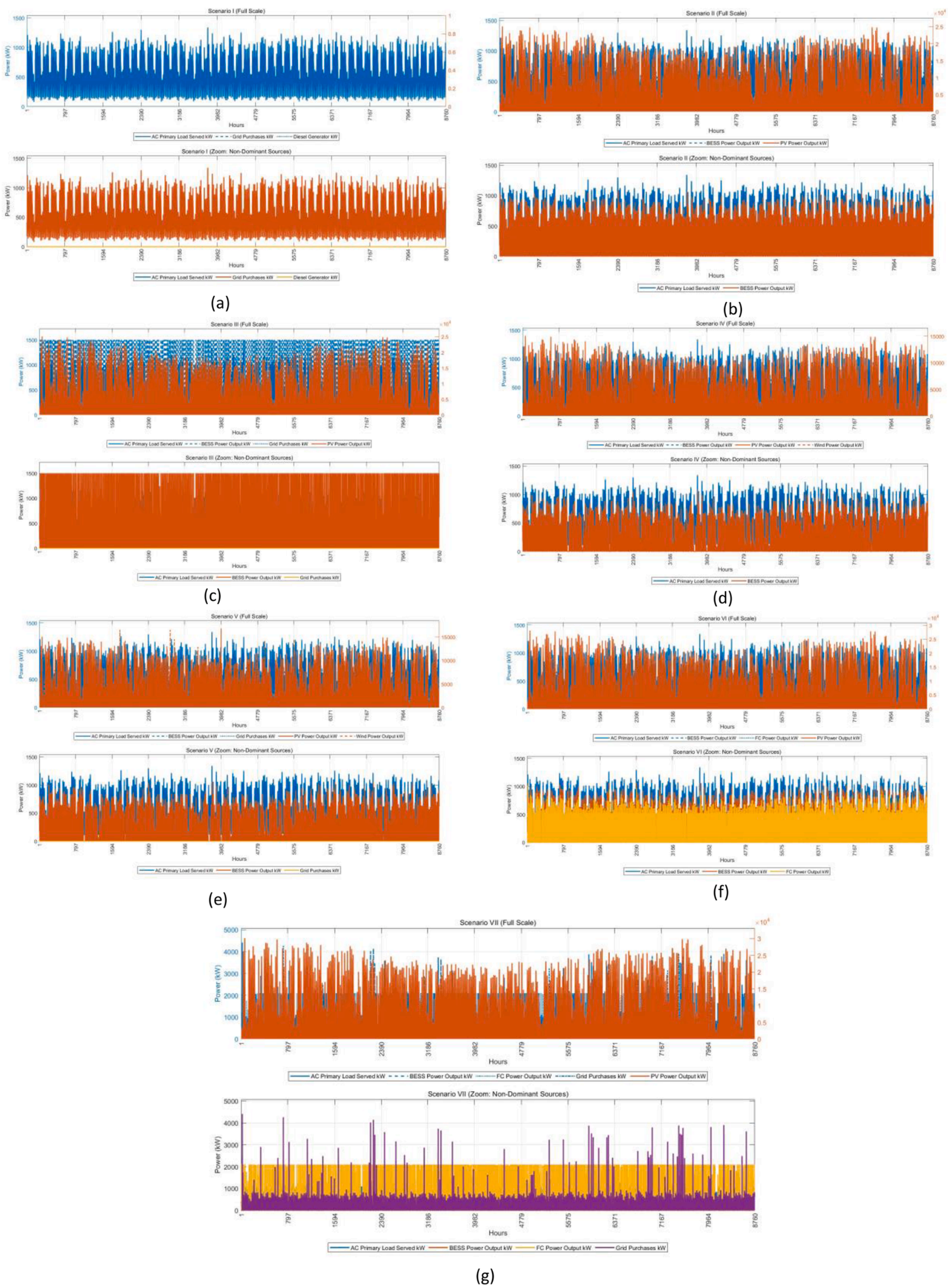

Fig. 10. Energy contribution of energy sources in scenarios (I-VII).

additional PV production. The produced hydrogen is stored in a 10,000 kg HT and then reconverted into electricity during periods of low production. This provides long-term and even seasonal storage capacity to meet energy demand that cannot be covered by batteries. By the end of the year, almost all of the hydrogen will have been used, indicating effective use of stored energy and a reduction in waste.

Scenario VII also maximizes the use of renewable energy and minimizes costs. As shown in Fig. 10, the PV system dominates the energy mix in all scenarios, providing the largest share compared to all other sources. This accounts for more than 90% of the annual supply, and the electrolyzer operates as a flexible load to absorb the additional production that would otherwise go unused in the pure BESS. This system exports 14.29 GWh annually to the grid while importing only 1.81 GWh per year, increasing energy autonomy and generating revenue opportunities through grid sales.

By balancing long-term and short-term storage, Scenario VII reduces the pressure and need for changes in BESS while maintaining high operational availability. Due to its ability to provide stable and continuous energy regardless of unfavourable resource conditions or grid interruptions, it is economically viable and robust compared to all other systems, concerning renewable integration and long-term energy security. In Scenario VII, the improved system achieves a levelised cost of hydrogen (LCOH) of $2.59/kg, which is very competitive compared to current global standards. According to literature, production costs for green hydrogen through electrolytic processes generally range between $4 and $6/kg in most markets, while particularly in areas with high availability of renewable resources and low electricity prices, lower prices are possible. It is important to note that the significance of hydrogen integration becomes more pronounced under the mixed campus load configuration. The presence of hostel demand during night-time hours reduces direct PV utilization and increases the reliance on stored energy. In contrast, an academic-only scenario would exhibit lower night-time demand, reducing hydrogen dispatch frequency and long-duration storage utilization. Therefore, the observed hydrogen production capacity and its effective annual utilization are directly linked to the comprehensive load modelling adopted in this study.

The LCOH in Scenario VII is not only below the current global average but also within the target corridor for 2030, predicted by the previous industry's roadmaps ($1.50–$3.00/kg) [22], indicating strong economic competitiveness under the modelled conditions. This low LCOH is mainly due to the electrolyzers being directly connected to the high PV energy production of the system and to the additional renewable energy production, which reduces electricity supply costs and avoids grid prices. Additionally, the efficient use of almost all the hydrogen produced through fuel cells increases the overall economic performance of the system, resulting in a decrease in the cost per unit of usable energy. In practice, all of this will depend on maintaining the high costs of renewable production, improving the efficiency factors of the electrolyzers, and minimizing losses during storage and distribution to reach $2.59 per kilogram. HOMER Pro applies deterministic component performance using fixed nominal efficiencies and does not explicitly model gradual electrolyzer stack degradation, part-load efficiency drift, or time-varying efficiency decay. Component end-of-life is represented through discrete replacement costing based on the specified lifetime. Therefore, the reported LCOH reflects nominal performance and should be interpreted as a best estimate under the assumed efficiencies; real-world degradation may increase the practical LCOH.

Although the modelled costs are promising, they assume perfect system coordination, higher utilization rates, and stable renewable production factors, which can be much more challenging in practice. Additional factors, such as the water supply for electrolysis, the long-term performance of the electrolyzer, and maintenance costs, must be taken into account when translating the results to practical projects. Hydrogen production through electrolysis requires water input, which represents an additional resource consideration for Scenarios VI and VII. Based on the annual hydrogen production of 560,078 kg, the estimated water requirement ranges between approximately 5,000–7,000 m^3 per year (assuming 9–12 liters of water per kg of hydrogen, including purification losses). While this demand is moderate relative to municipal-scale consumption, it introduces an important operational consideration, particularly in water-stressed regions. However, Scenario VII regarding the cost-performance relationship of hydrogen suggests that in areas with abundant solar energy and the appropriate infrastructure, green hydrogen may already approach the costs of green hydrogen in some markets, supporting its role as a long-term storage solution.

Table 7 compares the LCOH in different regions and highlights the significant cost advantages of hydrogen production from solar energy in the current study. In this case study, hydrogen production in Taxila, Pakistan, is carried out at an exceptionally low price of $2.59 per kilogram. In contrast, hydrogen production in other parts of the globe is comparatively higher. This shows the great potential for reducing hydrogen production costs through solar energy, as observed in this case study.

A comparative evaluation with existing literature demonstrates the strong economic competitiveness of the proposed HES. The LCOE achieved in the present study (0.0751 $/kWh) is substantially lower than those reported for analogous configurations across the Asian region, including Cambodia (0.257 $/kWh), Laos (0.265 $/kWh), Myanmar (0.269 $/kWh), and Bangladesh (0.271 $/kWh) [69], all of which depend primarily on conventional PV-DG-BESS architectures. The proposed system outperforms these benchmarks by margins ranging from 72% to 72.3%, underscoring the cost advantage offered by the Grid-PV-FC-BESS-Electrolyzer-HT configuration adopted in this work. Furthermore, even technologically advanced deployments such as those reported in South Korea (0.673 $/kWh) [70] and Thailand (0.728 $/kWh) [71] exhibit costs nearly an order of magnitude higher, confirming that the proposed system delivers a highly favorable economic outcomes.

Within the Pakistan-specific context, a previously reported LCOE of 0.078 $/kWh [72] represents the closest benchmark, yet the present study achieves a further reduction to 0.0751 $/kWh while simultaneously incorporating hydrogen-based components, namely FCs, electrolyzer, and HT, that were absent in the prior configuration. This integration introduces a layer of technological sophistication beyond that of conventional PV-BESS-DG systems, enabling enhanced energy storage flexibility, improved resilience under grid instability, and long-duration dispatch capability through hydrogen as a secondary energy carrier. Consequently, the proposed system not only advances the cost frontier for HRES in Pakistan but also establishes a more robust and future-oriented framework, validating both its economic efficiency and its potential as a replicable model for energy transition in developing economies with similar resource profiles.

4.1. Policy recommendations

Based on the results of the study, a few policy recommendations can be provided that are supported by the results of the study.

- Considering the results of the study in Scenarios, the Government should provide financial incentives (such as subsidies, tax rebates,

Table 7
Comparison of LCOH of scenario VII with different systems in the world.

Location	Country	LCOH ($/kg)
Tabriz, Khorasan, Esfahan, Zahedan [22]	Iran	In the range of 4.9 and 5.9
Nigde [94]	Türkiye	6.15
Zaragoza [95]	Spain	5.83
Aksaray [94]	Türkiye	21.5
Dhofar region [96]	Oman	5.67
Dakhla-Oued Ed-Dahab [97]	Morocco	3.30
Nadi [98]	Fiji	8.73
Taxila [Present Study]	Pakistan	2.59

and grants) to establish HRES for educational institutions, businesses, and communities to level up the clean energy initiative. For instance, Scenario VII utilized diverse energy sources, and the most cost-effective and sustainable solution is achieved. These benefits can potentially attract unconnected rural communities, industrial areas, and university campuses, which have the greatest need for clean and reliable energy solutions.

- It is recommended that policymakers set creative employment goals related to training programs and renewable energy technologies. Community development, the improvement of technical skills, and local jobs will benefit from these measures. An excellent example of HRES is that around 30 jobs are generated annually in Scenario VII for the project life lifetime, which helps promote economic development and improve quality of life, showing the larger projects have more potential to create Job opportunities.
- The hydrogen components in scenarios VI and VII are necessary to ensure that these hybrid renewable energy systems are fully renewable, and they are also essential for ensuring the efficiency of energy storage and supply. Integrating hydrogen production through electrolysis and fuel cells into these systems offers key benefits for addressing the intermittent nature of solar and wind energy, which are two main characteristics of renewable energy sources. For instance, in this study, Scenario VI has LCOH at 5.15 $/kg and in Scenario VII the LCOH is at 2.59 $/kg which is very low, therefore, by leveraging the excess solar energy during daytime hydrogen can be produced at a comparatively lower rates which would further drive the clean energy initiative.

5. Conclusion

To further expedite the clean energy initiative this research has explored different hybrid renewable energy system configurations for load of educational institutions. The results of the research show that HRES cannot only meet load needs but also maintain sustainability and reliability. Several key insights were obtained about the capacity and improvement of renewable energy systems in different scenarios from techno-economic, environmental, social, robustness, and sensitivity analyses. The results indicate that reliable and cost-effective energy solutions can be developed by combining solar photovoltaic systems, energy storage, and other renewable energy sources such as wind and fuel cells. Scenario I which is the base case includes a DG and a grid. Without producing additional energy or with no capacity limits, this configuration uses 5,005,975 kWh of grid energy each year. The NPC of this Scenario is $9.51 million and LCOE is $0.0856/kWh. This system emits 3,163,776 kg of CO_2 per year, making it the most polluting in all scenarios although it provides a constant energy source. It serves as a benchmark for comparison with more environmentally friendly options.

The NPC of Scenario II consisting of PV with BESS is $22.3 million and its LCOE is 0.2008 $/kWh. This system does not emit CO_2 because it is completely renewable, even though NPC and LCOE are high. This system generates 38,997,768 kWh annually, meeting all load demand using solar energy and the energy stored in BESS. However, since the lifespan of BESS is only five years the cost of energy is high and significantly more resources are spent on the transition. Scenario III consists of grid, the BESS, and solar PV energy. By selling 2,724,533 kWh of energy annually, this hybrid solution provides a more balanced approach to selling additional energy back to the grid. The NPC of this system is approximately $37 million and its LCOE is $0.215/kWh. The inclusion of grid connectivity allows for a more efficient use of energy and storage, reducing the total dependence on energy stored in the BESS, although the system's emissions remain zero.

In Scenario IV (wind energy, solar PV, and BESS), the diversification of the power generation system has increased. According to this scenario, the annual energy production is 25,384,496 kWh (92.2% from solar PV and 7.82% from wind energy) with an LCOE of $0.346/kWh and an NPC of $38.5 million. Despite the low cost, the wind component raises prices, as the installation and maintenance of wind turbines are expensive. Compared to Scenario I, the annual CO_2 emissions of this system are 1,127,240 kg, showing how the integration of renewable energy can benefit the environment. In Scenario V, solar PV energy, wind energy, BESS, and the electrical grid were included.

Of the total energy, 82.2% comes from the sun and 17.4% from the wind, generating a total of 25,384,496 kWh annually. Its LCOE is $0.289/kWh and its NPC is $70.1 million. Although the excess electricity is sold to the grid, it is not economically as beneficial compared to other renewable solutions due to the high cost of large BESS systems and additional wind turbines. In scenario VI, FC, electrolyzer, and HT were combined with PV and BESS. This configuration produces 44,959,939 kWh of energy annually, with an NPC of $42.5 million and an LCOE of $0.383/kWh.

Although its cost is higher, this system produces hydrogen from excess solar energy, providing a notable carbon saving, resulting in no CO_2 emissions. The best configuration, Scenario VII, includes the grid, photovoltaic solar energy, fuel cell, BESS, electrolysis, and hydrogen tank. It produces 50,838,592 kWh of energy annually, with an LCOE of $0.0751/kWh and an NPC of $32.18 million. Compared to Scenario I, the costs of this scenario are much lower, and its renewable energy share is 90.6%. It provides the best combination of reliability, affordable cost, and environmental sustainability. Additionally, in Scenario VI, the LCOH, which considers the costs of hydrogen production and storage, is $5.15/kg. In Scenario VII, thanks to the successful integration of solar energy for hydrogen production, the LCOH is significantly reduced to $2.59/kg, making it a more economical and environmentally friendly option for long-term energy storage. The achieved LCOH of $2.59/kg establishes a practical benchmark for developing countries, demonstrating that green hydrogen integration in campus-scale hybrid renewable systems can be economically competitive under favourable solar conditions. Based on the results of the techno-economic, environmental, social, and robustness analyses, it can be concluded that hybrid energy systems offer a cost-effective and environmentally friendly way to generate electricity. The transition to clean energy can be accelerated by producing low-cost hydrogen using additional solar energy. This approach not only reduces costs but also improves process efficiency, increasing the viability and effectiveness of the transition to green energy sources. Some suggestions for future research include focusing on real-world pilot projects, integrating with intelligent control systems, with special emphasis on clean energy systems based on hydrogen, and considering life cycle assessments to improve the technical, economic, and environmental feasibility of hybrid renewable energy systems. Additionally, future research should focus on modelling potential hydrogen resources in various climatic zones, evaluating policy and regulatory scenarios, and developing multidimensional decision-making frameworks that support the cost-effective integration of hydrogen technologies within the institutional context.

The optimal configuration requires 30 MW of PV, which has implications for physical siting and land availability. Utility-scale PV typically requires approximately 4–5 acres per MW (depending on module efficiency, tilt, and spacing), implying an estimated footprint of ~120–150 acres (≈0.49–0.61 km^2) for 30 MW. Although the total land area of UET Taxila is approximately 163 acres, this includes academic facilities, roads, green space, hostels, and faculty housing; therefore, only a fraction of the site is practically available for ground-mounted PV deployment. Consequently, the proposed PV capacity should be interpreted as a campus-supply target that can be achieved through a hybrid installation strategy, including rooftop PV on academic buildings and hostels, solar canopies over parking and walkways, and limited ground-mounted arrays on available open land or adjacent parcels near the campus boundary. This approach improves practical feasibility while maintaining the optimized techno-economic benefits of Scenario VII. Therefore, University will need to lend the adjacent land to university for PV installation. Figure A3 in the appendix presents the land estimation for PV installation. Furthermore, HOMER Pro employs deterministic optimization based on historical weather and load data, which assumes perfect foresight and does not fully capture real-time operational uncertainties such as sudden weather variability, load fluctuations, or equipment outages.

The applicability of this study is largely defined by its specific local context, meaning the favourable results for Scenario VII may not hold in regions with different solar resources, grid characteristics, or economic policies such as feed-in tariffs and inflation rates. The system's profitability is highly sensitive to these external factors, particularly regarding the capital-intensive nature of hydrogen technology and the volatility of energy export prices. Beyond the economics, practical implementation on university campuses faces significant hurdles, including strict safety regulations, space limitations, and the necessity of managing the entire hydrogen lifecycle on-site due to a lack of external infrastructure. To address these challenges, future adoption should prioritize modular, scalable designs that allow for gradual investment, leveraging industry partnerships and existing facilities to navigate both the financial and logistical barriers of hydrogen integration. Although the optimized configuration allows significant grid export, practical implementation would require compliance with IESCO interconnection standards and export capacity limits. The present analysis assumes grid absorption capability as modeled in HOMER Pro; however, detailed distribution network studies would be required to confirm export feasibility under real operating conditions. Future research could investigate the integration of flexible and shiftable loads, such as university data centers, within the campus microgrid to enhance renewable energy utilization and reduce curtailment. Coordinating computing workload migration with energy storage systems, as demonstrated in recent studies [73,74] may further improve operational efficiency and decarbonization potential in campus-scale hybrid systems. Future work should extend the current sensitivity-based approach by adopting stochastic optimization to capture both exogenous variability (weather, prices) and endogenous uncertainties, such as decision-dependent demand response [75]. Future studies could leverage the campus's substantial residential demand by exploiting building thermal inertia as a flexibility resource. Coordinated aggregation of space-heating/thermal loads may flatten peak demand and reduce the required sizing of both battery and hydrogen storage systems [76,77]. Future work could enhance risk assessment accuracy by moving beyond standard Gaussian assumptions for load and solar variability and adopting data-driven uncertainty modeling techniques. Approaches such as kernel density estimation, as demonstrated by Giannelos et al. [78], would enable a more realistic representation of non-Gaussian uncertainties in campus energy hub operation.

CRediT authorship contribution statement

Asjad Ali: Writing – original draft, Software, Methodology, Data curation, Conceptualization. **Noor Izzri Abdul Wahab:** Visualization, Validation, Supervision. **Zain Ul Abdeen Qureshi:** Writing – review & editing, Investigation, Formal analysis. **Usama Azmat:** Validation, Formal analysis, Data curation. **Hafiz Abdul Muqeet:** Validation, Project administration, Data curation. **Reihaneh Aghamolaei:** Writing – review & editing, Validation, Methodology.

Declaration of competing interest

The authors declare that they have no known competing financial interests or personal relationships that could have appeared to influence the work reported in this paper.

Appendix

$$C_{total} = CRF(i_r, T_y) \times TNPC \tag{A1}$$

$$\text{Capital Recovery Factor } (CRF(i_r, T_y)) = \frac{i_r(1 + i_r)^{T_y}}{(1 + i_r)^{T_y} - 1} \tag{A2}$$

$$E_{DG} = \sum_{j=1}^{n} E_{DG(j\ldots n)} \tag{A3}$$

$$C_{grid} = \sum_{\text{rates } r} \sum_{m=1}^{12} (P_{demand,r,m} . C_{demand,r}) \tag{A4}$$

$$T_{Total} = T_{AEC} + C_{grid} \tag{A5}$$

$$\sum_{\text{rates } r} \sum_{m=1}^{12} (E_{sell,r,m} .\ C_{sell,r})\ \text{kWh} \Big/ \text{year} \tag{A6}$$

$$T_{Total} = \sum_{\text{rates } r} \sum_{m=1}^{12} (E_{buy,peak,r,m} .\ C_{buy,peak,r} + E_{buy,non-peak,r,m} .\ C_{buy,non-peak,r}) - \sum_{\text{rates } r} \sum_{m=1}^{12} (E_{sell,peak,r,m} .\ C_{sell,peak,r} + E_{sell,non-peak,r,m} . C_{sell,non-peak,r,m}) \tag{A7}$$

$$SOC_{bat}^{min} = (1 - DOD_{bat}) \times Cp_{\ batt} \tag{A8}$$

$$F_{DG}(t) = P_{DG}(t) \times \left(a + b \times \frac{P_{DG}(t)}{P_{rated}}\right) \tag{A09}$$

$$E_{emission} = F_{DG}(t) \times \text{ Emission Factor} \tag{A10}$$

$$P_{htank} = \left(\frac{RT_{htci}}{V_{Htank}}\right) \text{nHtank} \tag{A11}$$

$$A_{Ht} = \left[\frac{C_{Ht} LVH \left(\frac{24h}{d} \right)}{La.p \left(\frac{3.6MJ}{kWh} \right)} \right] \tag{A12}$$

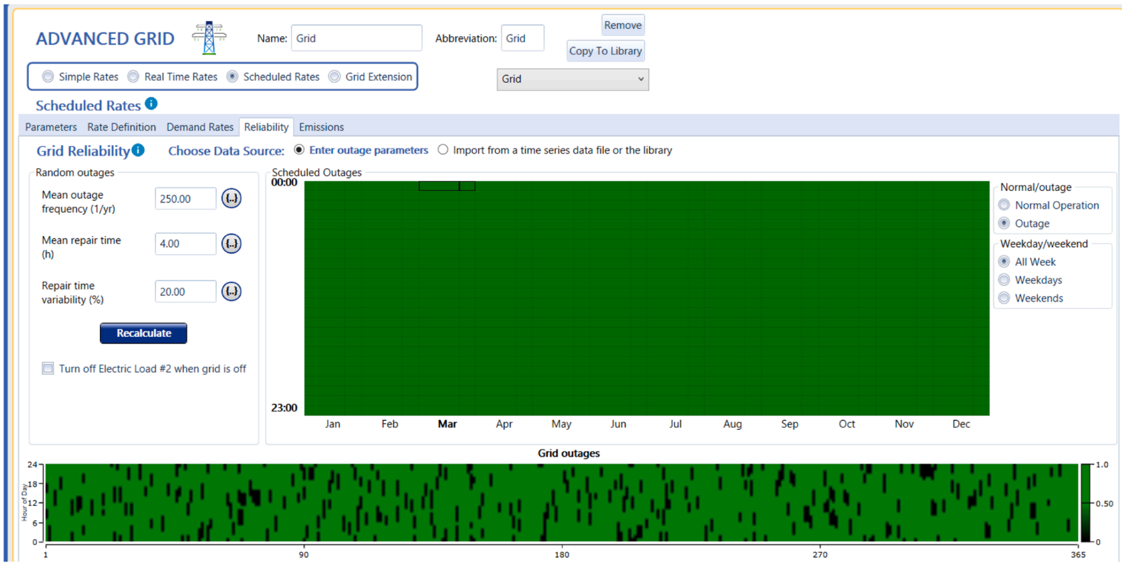

Fig. A1. Grid reliability with probabilistic outages.

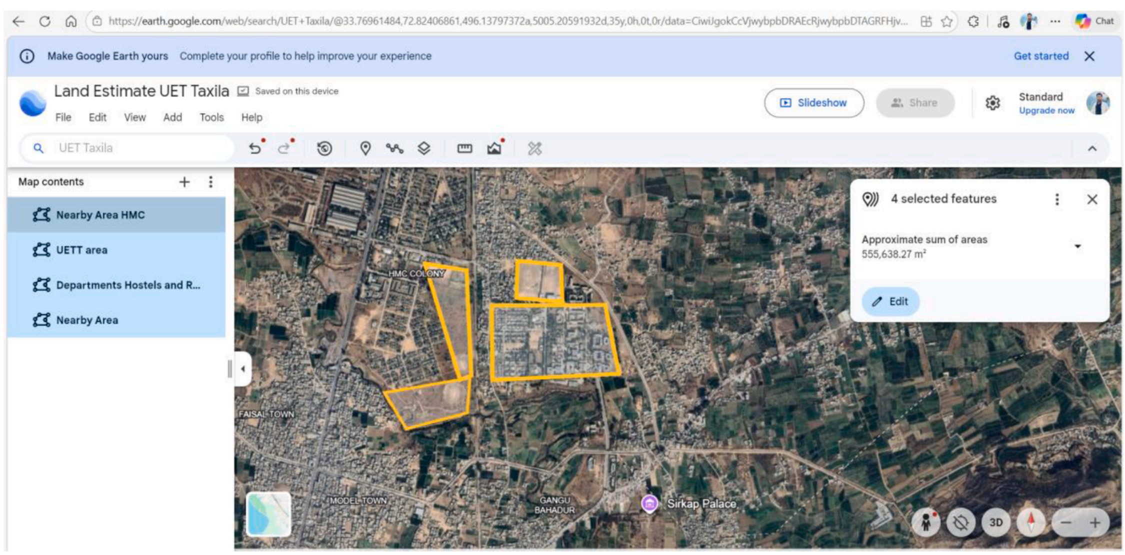

Fig. A2. Land calculation for PV installation for optimal scenario VII.

Table A1
Configuration for formation of multiple hybrid scenarios.

Scenarios	Switches Condition: ✔ shows component is connected							
	S1	S2	S3	S4	S5	S6	S7	S8
Scenario I	✔		✔					
Scenario II				✔	✔			
Scenario III	✔			✔	✔			
Scenario IV		✔		✔	✔			
Scenario V	✔	✔		✔	✔			
Scenario VI				✔	✔	✔	✔	✔
Scenario VII	✔			✔	✔	✔	✔	✔

Table A2
Technical parameters and costs of different components in HRES [66].

Parameters	Value	Units
PV panel (LONGI Solar LR6–72PE)		
Capacity	750	W
Capital Cost	259	$
Replacement Cost	185	$
O&M Cost	3.37	$/yr
Temp. effect	0.38	%/ °C
Efficiency	24.1	%
Lifetime	25	Year(s)
DE rating	0.05	%/year
Wind turbine (Generic 10 kW)		
Capacity	10	kW
Capital Cost	15,000	$/kW
Replacement Cost	12,500	$/kW
O&M cost	100	$/yr
Lifetime	25	Year(s)
Hub height	24	M
Battery (Generic 1 kWh **Li-ion)**		
Nominal capacity	1	kWh
Capital	200	$/kW
Replacement Cost	200	$/kW
O&M Cost	10	$/yr
Lifetime	5	Year(s)
Efficiency	90	%
Electrolyzer		
Considered size for optimization	8000, 10000, 12000	kW
Capital Cost	1100	$/kW
Replacement Cost	850	$/kW
O&M Cost	10	$/yr
Lifetime	25	Year(s)
Efficiency	85	%
Diesel Generator		
Capacity	600	kW
Capital Cost	none	$
Replacement Cost	250,000	$
O&M Cost	0.030	$/op. hour
Lifetime	15,000	h
Efficiency	85	%
Fuel cell (Auto-size)		
Capacity	2100	kW
Capital Cost	2000	$/kW
Replacement Cost	2000	$/kW
O&M cost	0	$/h
Lifetime	15,000	h
Efficiency	85	%
Converter (Auto-size)		
Capacity	HOMER Optimization	kW
Capital	150	$/kW
Replacement cost	150	$/kW
O&M cost	10	$/yr
Lifetime	15	Year(s)
Efficiency	95	%
Hydrogen tank		
Considered size for optimization	10000,13000,15000	kg
Capital cost	600	$/kW
Replacement cost	600	$/kW
O&M cost	10	$/yr
Lifetime	25	Year(s)
Initial tank level w.r.t tank size	30	%

Table A3
Load 1 – residential + hostels.

Appliance	Quantity	Rating (W)	Avg. Operating Hours	Energy Consumption (kWh/day)
Lights	5,000	15	6	450
Fans	3,000	70	8	1,680
TV	1,000	100	4	400
Refrigerators	800	150	24	2,880
Water Motors	400	750	1	300
Phone Chargers	5,000	5	5	125
Irons	600	1,000	0.5	300
Washing Machines	250	500	1.5	187.5

(*continued on next page*)

Table A3 (*continued*)

Appliance	Quantity	Rating (W)	Avg. Operating Hours	Energy Consumption (kWh/day)
Room Heaters	100	2,000	4	800
Total Load 1				8,550

Table A4
Load 2 – departments.

Appliance	Quantity	Rating (W)	Avg. Operating Hours	Energy Consumption (kWh/day)
Lights	8,000	20	7	1,120
Fans	1500	80	8	960
Desktop PCs	1800	250	5	2,250
Projectors	200	300	2	120
Air Conditioners	120	2,000	2	480
Lab Equipment	200	500	2	200
Printers	90	200	2	36
Total Load 2				5165

Table A5
Combined daily load summary.

Category	Daily Load (kWh/day)
Load 1 (Hostels + Residential)	8,550.0
Load 2 (Departments)	5,165.0
Grand Total	15,240.0

Table A6
Optimization settings.

System Settings	Values	Source of Information
Design Precision	0.01	General information obtained from HOMER Pro [79]
Simulation time step	1 h	Default settings in HOMER Pro [79]
Inflation rate	7%	The official website of the State Bank of Pakistan [80]
Life Time of System	15 years	Generic Settings [79]
Capacity Shortage	0 %	Generic setting [79]
CO2 Penalty	0	Generic Settings [79]
Nominal Discount Rates	8%	The official website of the State Bank of Pakistan [80]

Table A7
Cost breakdown of different energy sources in scenario I.

Costs ($)	Grid	Diesel Gen	System
Capital Cost	0	0	0
Replacement Cost	0	0	0
O&M Cost	9.51018E6	0	9.51018E6
Fuel Cost	0	0	0
Salvage	0	−193172.45	−193172.45
Total	9.51018E6	−193172.45	9.317E6
Capital Cost	0	0	0

Table A8
Cost breakdown of different energy sources in scenario II.

Costs ($)	Battery Storage System	Solar PV	Power Converter	System
Capital Cost	2.3456E6	6.475E6	210570.29	9.03117E6
Replacement Cost	8.36375E6	0	183146	8.5469E6
O&M Cost	2.60388E6	1.87054E6	311675.61	4.78609E6
Fuel Cost	0	0	0	0
Salvage	0	0	−55625.82	−55625.82
Total	1.33132E7	8.34554E6	649766.08	2.23085E7
Capital Cost	2.3456E6	6.475E6	210570.29	9.03117E6

Table A9
Cost breakdown of different energy sources in scenario III.

Costs ($)	Battery Storage System	Solar PV	Power Converter	System
Capital Cost	2.3456E6	6.475E6	210570.29	9.03117E6
Replacement Cost	8.36375E6	0	183146	8.5469E6
O&M Cost	2.60388E6	1.87054E6	311675.61	4.78609E6
Fuel Cost	0	0	0	0
Salvage	0	0	−55625.82	−55625.82
Total	1.33132E7	8.34554E6	649766.08	2.23085E7
Capital Cost	2.3456E6	6.475E6	210570.29	9.03117E6

Table A10
Cost breakdown of different energy sources in scenario IV.

Costs ($)	Battery Storage System	Solar PV	Wind Turbines	Grid	Power Converter	System
Capital Cost	3.2E6	3.885E6	1.089E7	0	212639.44	1.81876E7
Replacement Cost	1.14103E7	0	7.53437E6	0	184945.66	1.91296E7
O&M Cost	3.55236E6	1.12232E6	1.61188E6	−8.11278E6	314738.25	6.60131E6
Fuel Cost	0	0	0	0	0	0
Salvage	0	0	−5.39397E6	0	−56172.42	−5.45014E6
Total	1.81627E7	5.00732E6	1.46423E7	−8.11278E6	656150.93	3.84684E7
Capital Cost	3.2E6	3.885E6	1.089E7	0	212639.44	1.81876E7

Table A11
Cost breakdown of different energy sources in scenario V.

Costs ($)	Battery Storage System	Solar PV	Wind Turbines	Power Converter	System
Capital Cost	3.2E6	3.885E6	1.089E7	212639.44	1.81876E7
Replacement Cost	1.14103E7	0	7.53437E6	184945.66	1.91296E7
O&M Cost	3.55236E6	1.12232E6	1.61188E6	314738.25	6.60131E6
Fuel Cost	0	0	0	0	0
Salvage	0	0	−5.39397E6	−56172.42	−5.45014E6
Total	1.81627E7	5.00732E6	1.46423E7	656150.93	3.84684E7
Capital Cost	3.2E6	3.885E6	1.089E7	212639.44	1.81876E7

Table A12
Cost breakdown of different energy sources in scenario VI.

Costs ($)	Battery Storage System	Solar PV	Hydrogen Tank	Electrolyzer	Fuel Cell	Grid	Power Converter	System
Capital Cost	800000	7.77E6	6E6	8.8E6	4.2E6	0	1.78469E6	2.93547E7
Replacement Cost	2.85258E6	0	0	0	0	0	1.55226E6	4.40483E6
O&M Cost	888089.97	2.24465E6	2.22022E6	1.77618E6	1.60016E6	−9.78336E6	2.64161E6	1.58756E6
Fuel Cost	0	0	0	0	0	0	0	0
Salvage	0	0	0	0	−2.69387E6	0	−471457.42	−3.16533E6
Total	4.54067E6	1.00146E7	8.22022E6	1.05762E7	3.10629E6	−9.78336E6	5.5071E6	3.21817E7
Capital Cost	800000	7.77E6	6E6	8.8E6	4.2E6	0	1.78469E6	2.93547E7

Table A13
Cost breakdown of different energy sources in scenario VII.

Costs ($)	Battery Storage System	Solar PV	Hydrogen Tank	Electrolyzer	Fuel Cell	Power Converter	System
Capital Cost	800000	7.252E6	9E6	8.8E6	4.2E6	196607.81	3.02486E7
Replacement Cost	2.85258E6	0	0	0	0	171001.97	3.02358E6
O&M Cost	888089.97	2.095E6	3.33034E6	1.77618E6	3.02408E6	291009.04	1.14047E7
Fuel Cost	0	0	0	0	0	0	0
Salvage	0	0	0	0	−2.12914E6	−51937.38	−2.18107E6
Total	4.54067E6	9.347E6	1.23303E7	1.05762E7	5.09494E6	606681.44	4.24958E7
Capital Cost	800000	7.252E6	9E6	8.8E6	4.2E6	196607.81	3.02486E7

Table A14
Search space limitations of components.

		Scenario I	Scenario II	Scenario III	Scenario IV	Scenario V	Scenario VI	Scenario VII
PV (kW)		-	0-2000-25000	0-20000-25000	0-15000	0-10000-15000	0-20000-28000	0-10000-20000-30000
Wind (kW)		-	-	-	HOMER Optimizer	HOMER Optimizer	-	-
BESS (Strings)		-	HOMER Optimizer	HOMER Optimizer	0-2000	0-4000	0-500	0-500
Grid (kW)	Purchase Capacity	999999	-	999999	-	999999	999999	999999
	Sales Capacity	999999	-	999999	-	999999	999999	999999
Hydrogen Storage	-	-	-	-	-	-	0-10000-12000-15000	0-10000-13000-15000
Electrolyzer		-	-	-	-	-	7500-8000	8000-10000-12000
Fuel Cell	-	-	-	-	-	-	HOMER Optimizer	HOMER Optimizer

Data availability

Data will be made available on request.

References

[1] A. Buonomano, G. Barone, C. Forzano, Latest advancements and challenges of technologies and methods for accelerating the sustainable energy transition, Energy Rep. 9 (2023) 3343–3355, https://doi.org/10.1016/j.egyr.2023.02.015.
[2] S. Ahmad, A review of microgrid energy management and control strategies, IEEE Access 11 (January) (2023) 21729–21757, https://doi.org/10.1109/ACCESS.2023.3248511.
[3] A. Ali, et al., Optimizing renewable energy integration : a hybrid energy system approach for residential applications, in: International Conference on Energy, Power, Environment, Control and Computing, ICEPECC, 2025, pp. 1–8.
[4] T.F. Agajie, et al., A comprehensive review on techno-economic analysis and energy storage systems, Energies 16 (642) (2023) 1–26.
[5] S. Kirsch, The extractive industries and society running out ? rethinking resource depletion, Extr. Ind. Soc. 7 (3) (2020) 838–840, https://doi.org/10.1016/j.exis.2020.06.002.
[6] M. Khalid, Smart grids and renewable energy systems: perspectives and grid integration challenges, Energy Strateg. Rev. 51 (June 2023) (2024) 101299, https://doi.org/10.1016/j.esr.2024.101299.
[7] A.Q. Al-Shetwi, Sustainable development of renewable energy integrated power sector: trends, environmental impacts, and recent challenges, Sci. Total Environ. 822 (2022) 153645, https://doi.org/10.1016/j.scitotenv.2022.153645.
[8] Y.G. Son, B.C. Oh, M.A. Acquah, R. Fan, D.M. Kim, S.Y. Kim, Multi energy system with an associated energy hub: a review, IEEE Access 9 (2021) 127753–127766, https://doi.org/10.1109/ACCESS.2021.3108142.
[9] S. Kanwal, M.T. Mehran, M. Hassan, M. Anwar, S.R. Naqvi, A.H. Khoja, An integrated future approach for the energy security of Pakistan: replacement of fossil fuels with syngas for better environment and socio-economic development, Renew. Sustain. Energy Rev. 156 (April 2021) (2022) 111978, https://doi.org/10.1016/j.rser.2021.111978.
[10] T. Aized, S.M.S. Rehman, M. Sumair, Pakistan energy situation, policy, and issues, Elsevier Inc., 2021, https://doi.org/10.1016/B978-0-323-91093-4.00011-1.
[11] A. Ali, et al., Optimal μ -PMU placement and voltage estimation in distribution networks : evaluation through multiple case studies, Sustain 17 (24) (2025) 11036, https://doi.org/10.3390/su172411036.
[12] A.Q. Al-Shetwi, M.A. Hannan, K.P. Jern, M. Mansur, T.M.I. Mahlia, Grid-connected renewable energy sources: review of the recent integration requirements and control methods, J. Clean. Prod. 253 (2020) 119831, https://doi.org/10.1016/j.jclepro.2019.119831.
[13] T. Kataray, et al., Integration of smart grid with renewable energy sources: opportunities and challenges – a comprehensive review, Sustain. Energy Technol. Assessments 58 (March) (2023) 103363, https://doi.org/10.1016/j.seta.2023.103363.
[14] Y. Tahir, M.F. Nadeem, A. Ahmed, I.A. Khan, F. Qamar, A review on hybrid energy storage systems in microgrids, in: 2020 3rd Int. Conf. Comput. Math. Eng. Technol. Idea to Innov. Build. Knowl. Econ. iCoMET 2020, 2020, pp. 0–6, https://doi.org/10.1109/iCoMET48670.2020.9073919.
[15] H.A. Muqeet, et al., Sustainable solutions for advanced energy management system of campus microgrids: model opportunities and future challenges, Sensors 22 (6) (2022) 2345, https://doi.org/10.3390/s22062345.
[16] A. Ali, "Single objective hybrid PSOGWO algorithm for optimal micro-PMU placement," *2025 3rd Power Electron. Power Syst. Conf.*, pp. 105–110, doi: 10.1109/PEPSC67251.2025.11453325.
[17] S.M. Dawoud, X. Lin, M.I. Okba, Hybrid renewable microgrid optimization techniques : a review, Renew. Sustain. Energy Rev. 82 (August 2017) (2018) 2039–2052, https://doi.org/10.1016/j.rser.2017.08.007.
[18] I. J. Of and I. Revolution, Innovation and assessing feasibility studies on smart microgrid systems : a global review and methodological comparison for implementing microgrids in Malaysia, Int. J. Innov. Ind. Revolut. 5 (13) (2023) 20–27, https://doi.org/10.35631/IJIREV.513003.
[19] M.E.H. Mobi Mathew, Md Shafayet Hossain, Sajeeb Saha, Som Mondal, Sizing approaches for solar photovoltaic-based microgrids: a comprehensive review, IET Energy Syst. Integr. 4 (1) (2022) 1–27, https://doi.org/10.1049/esi2.12048.
[20] S. Kılıç Depren, M.T. Kartal, N.Çoban Çelikdemir, Ö. Depren, Energy consumption and environmental degradation nexus: a systematic review and meta-analysis of fossil fuel and renewable energy consumption, Ecol. Inform. 70 (June) (2022) 101747, https://doi.org/10.1016/j.ecoinf.2022.101747.
[21] B. Novotnik, et al., Can fossil fuel energy be recovered and used without any CO2 emissions to the atmosphere? Rev. Environ. Sci. Biotechnol. 19 (1) (2020) 217–240, https://doi.org/10.1007/s11157-020-09527-z.
[22] S. Shahabaddin, H. Dehshiri, B. Firoozabadi, Hydrogen penetration in textile industry : a hybrid renewable energy system, evolution programming and feasibility analysis, Energy 318 (August 2024) 2025.
[23] A. Ali, N. Izzri, A. Wahab, M.L. Othman, R.A. Farade, State estimation by optimal micro-PMU placement in radial distribution network, in: 2025 IEEE Int. Conf. Energy Technol. Futur. Grids, 2025, pp. 1–6, https://doi.org/10.1109/ETFG61999.2025.11402452.
[24] S. Nazir, A. Ali, A. Aftab, H.A. Muqeet, S. Mirsaeidi, J. Zhang, Techno-economic and environmental perspectives of solar cell technologies : a comprehensive review, Energies (2023) 1–32.
[25] A. Kumar, et al., Hybrid solar-wind energy system with storage provision and solar panel tracking to empower sustainable electrification, Next Res. 7 (February) (2026).
[26] K.K. Saini, P. Sharma, H.D. Mathur, A.R. Gautam, R.C. Bansal, Techno-economic and reliability assessment of an off-grid solar-powered energy system, Appl. Energy 371 (May) (2024) 123579, https://doi.org/10.1016/j.apenergy.2024.123579.
[27] M.S. Bakare, A. Abdulkarim, M. Zeeshan, A.N. Shuaibu, A comprehensive overview on demand side energy management towards smart grids: challenges, solutions, and future direction, Energy Inform. 6 (1) (2023), https://doi.org/10.1186/s42162-023-00262-7.
[28] H.A. Muqeet, R. Liaqat, M. Jamil, A.A. Khan, A state-of-the-art review of smart energy systems and their management in a smart grid environment, Energies 16 (1) (2023) 472, https://doi.org/10.3390/en16010472.
[29] M.S. Akhter, A review on various optimal microgrid sources and modelling using HOMER, in: IC-RTETM-2022 Organized by GGSF's GGS Polytechnic, Nashik, 2022.
[30] P.T. Kosmas, A. Kavadias, Hybrid renewable energy systems ' optimisation. a review and extended comparison of the most-used software tools, Energies 14 (24) (2021) 8268.
[31] I. Kapungwe and E. Bayram, "Demand side management in smart grids," pp. 5–9, 2020.
[32] R. Burian, M. Gontijo, H. Alvarez, Robustness and reliability in smart grid solutions, in: Proc. 2019 7th Int. Conf. Smart Energy Grid Eng. SEGE 2019, 2019, pp. 59–62, https://doi.org/10.1109/SEGE.2019.8859947.
[33] A. Esmaeilzadeh, B. Deal, A. Yousefi-koma, and M. R. Zakerzadeh, "How multi-criterion optimized control methods improve effectiveness of multi-zone building heating system upgrading," 2022.
[34] S. Iqbal, et al., Feasibility study and deployment of solar photovoltaic system to enhance energy economics of King Abdullah Campus, University of Azad Jammu and Kashmir Muzaffarabad, AJK Pakistan, IEEE Access 10 (2022) 5440–5455, https://doi.org/10.1109/ACCESS.2022.3140723.
[35] H. Javed, H.A. Muqeet, M. Shehzad, M. Jamil, A.A. Khan, J.M. Guerrero, Optimal energy management of a campus microgrid considering financial and economic analysis with demand response strategies, Energies 14 (24) (2021) 8501, https://doi.org/10.3390/en14248501.
[36] T.M.I. Riayatsyah, T.A. Geumpana, I.M. Rizwanul Fattah, S. Rizal, T.M. Indra Mahlia, Techno-economic analysis and optimisation of campus grid-connected hybrid renewable energy system using HOMER grid, Sustain 14 (13) (2022) 7735, https://doi.org/10.3390/su14137735.

[37] O. Khaled, M. Zahid, T. Zahid, T. Ilahi, Techno-economic feasibility of hybrid energy systems installation in Pakistan, IEEE Access 12 (February) (2024) 41643–41658, https://doi.org/10.1109/ACCESS.2024.3376409.
[38] S.S. Mendu, P. Appikonda, A.K. Emadabathuni, N. Koritala, Techno-economic comparative analysis between grid-connected and stand-alone integrated energy systems for an educational institute, Evergr. Jt. J. Nov. Carbon Resour. Sci. Green Asia Strateg. 7 (3) (2020) 382–395, https://doi.org/10.5109/4068616.
[39] Y.B. Aemro, P. Moura, A.T. De Almeida, Design and modeling of a standalone Dc-Microgrid for off-grid schools in rural areas of developing countries, Energies 13 (23) (2020) 6379, https://doi.org/10.3390/en13236379.
[40] M.F. Ishraque, S.A. Shezan, J.N. Nur, M.S. Islam, Optimal Sizing and assessment of an islanded photovoltaic-battery-diesel generator microgrid applicable to a remote school of Bangladesh, Eng. Rep. 3 (1) (2021) 1–19, https://doi.org/10.1002/eng2.12281.
[41] N. Shirzadi, F. Nasiri, U. Eicker, Optimal configuration and sizing of an integrated renewable energy system for isolated and grid-connected microgrids: the case ofan Urban University campus, Energies 13 (3527) (2020) 3527, https://doi.org/10.3390/en13143527.
[42] L. Al-Ghussain, A. Darwish Ahmad, A.M. Abubaker, M.A. Mohamed, An integrated photovoltaic/wind/biomass and hybrid energy storage systems towards 100% renewable energy microgrids in university campuses, Sustain. Energy Technol. Assess. 46 (May) (2021) 101273, https://doi.org/10.1016/j.seta.2021.101273.
[43] H.A.U. Muqeet, A. Ahmad, Optimal scheduling for campus prosumer microgrid considering price based demand response, IEEE Access 8 (2020) 71378–71394, https://doi.org/10.1109/ACCESS.2020.2987915.
[44] F. Ahmad, M.S. Alam, Optimal sizing and analysis of solar PV, wind, and energy storage hybrid system for campus microgrid, Smart Sci. 6 (2) (2018) 150–157, https://doi.org/10.1080/23080477.2017.1417005.
[45] O.D. Ohijeagbon, O. Ajayi, O. Waheed, M. Adekojo, E.Y. Salawu, F.A. Oyawale, Design of optimal hybrid renewable energy system for sustainable power supply to isolated-grid communities in North Central, Nigeria, Procedia Manuf. 35 (2016) (2019) 278–284, https://doi.org/10.1016/j.promfg.2019.05.040.
[46] A. Alkassem, A. Draou, A. Alamri, H. Alharbi, Design analysis of an optimal microgrid system for the integration of renewable energy sources at a university campus, Sustain 14 (7) (2022) 4175, https://doi.org/10.3390/su14074175.
[47] “HOMER Pro 3.15.” [Online]. Available: https://homerenergy.com/products/pro/docs/3.15/how_homer_calculates_emissions.html.
[48] C. Alkalah, “Expanding Renewable Energy in Pakistan’s Electricity Mix.” [Online]. Available: https://www.worldbank.org/en/news/feature/2020/11/09/a-renewable-energy-future-for-pakistans-power-system.
[49] Z. Abdin, W. Mérida, Hybrid energy systems for off-grid power supply and hydrogen production based on renewable energy: a techno-economic analysis, Energy Convers. Manag. 196 (January) (2019) 1068–1079, https://doi.org/10.1016/j.enconman.2019.06.068.
[50] A. Chauhan, R.P. Saini, Techno-economic optimization based approach for energy management of a stand-alone integrated renewable energy system for remote areas of India, Energy 94 (2016) 138–156, https://doi.org/10.1016/j.energy.2015.10.136.
[51] B.S. Al-Sharafi, Ahmet Z. Abdullah, Ayar Sahin, Yilbasa Tahir, Techno-economic analysis and optimization of solar and wind energy systems for power generation and hydrogen production in Saudi Arabia, Sustain. Energy Rev. 69 (November 2016) (2017) 33–49, https://doi.org/10.1016/j.rser.2016.11.157.
[52] H. Bakhtiari and R. A. Naghizadeh, “Multi-criteria optimal sizing of hybrid renewable energy systems including wind, photovoltaic, battery, and hydrogen storage with ε-constraint method,” pp. 883–892, 2018, doi: 10.1049/iet-rpg.2017.0706.
[53] N. Ghorbani, A. Kasaeian, A. Toopshekan, L. Bahrami, A. Maghami, Optimizing a hybrid wind-PV-battery system using GA-PSO and MOPSO for reducing cost and increasing reliability, Energy 154 (2018) 581–591, https://doi.org/10.1016/j.energy.2017.12.057.
[54] “IESCO tariff 2024 – electricity new unit price.” [Online]. Available: https://www.iesco.com.pk/.
[55] S. Singh, M. Singh, S.C. Kaushik, Feasibility study of an islanded microgrid in rural area consisting of PV, wind, biomass and battery energy storage system, Energy Convers. Manag. 128 (2016) 178–190, https://doi.org/10.1016/j.enconman.2016.09.046.
[56] A.S. Aziz, M.F.N. Tajuddin, M.R. Adzman, A. Azmi, M.A.M. Ramli, Optimization and sensitivity analysis of standalone hybrid energy systems for rural electrification: a case study of Iraq, Renew. Energy 138 (2019) 775–792, https://doi.org/10.1016/j.renene.2019.02.004.
[57] S. Yadav, P. Kumar, A. Kumar, Techno-economic assessment of hybrid renewable energy system with multi energy storage system using HOMER, Energy 297 (April) (2024) 131231, https://doi.org/10.1016/j.energy.2024.131231.
[58] K.V. Konneh, O.B. Adewuyi, M.M. Gamil, A.M. Fazli, T. Senjyu, A scenario-based multi-attribute decision making approach for optimal design of a hybrid off-grid system, Energy 265 (2023) 125663, https://doi.org/10.1016/J.ENERGY.2022.125663.
[59] Z. Arifin, et al., Grid-connected hybrid PV-wind system simulation in urban java, J. Eur. Des Syst. Autom. 55 (4) (2022) 477–483, https://doi.org/10.18280/jesa.550406.
[60] Ed Kyle, “AWS HC E-5 DATA SHEET,” Ed Kyle. [Online]. Available: https://www.ryse.energy/5kw-wind-turbines/.
[61] A. Askarzadeh, S. Coelho, A novel framework for optimization of a grid independent hybrid renewable energy system : a case study of Iran, Sol. Energy 112 (2015) 383–396, https://doi.org/10.1016/j.solener.2014.12.013.
[62] P. Tiam, B. Astrid, M. Nouadje, V. Chegnimonhan, and G. Tchuen, “Techno-economic feasibility of a PV /battery /fuel cell / electrolyzer / biogas hybrid system for energy and hydrogen production in the far north region of cameroon by using HOMER pro,” vol. 44, no. July, 2022, doi: 10.1016/j.esr.2022.100988.
[63] A. Dargahi, Optimal household energy management using V2H flexibilities, Int. J. Comput. Math. Electr. Electron. Eng. 33 (3) (2014) 777–792, https://doi.org/10.1108/COMPEL-10-2012-0223.
[64] M.F.H. Mojumder, et al., Techno-economic and environmental analysis of hybrid energy systems for remote areas: a sustainable case study in Bangladesh, Energy Convers. Manag. X 23 (April) (2024) 100664, https://doi.org/10.1016/j.ecmx.2024.100664.
[65] Z. Serat, M. Danishmal, F.Mohammad Mohammadi, Optimizing hybrid PV/Wind and grid systems for sustainable energy solutions at the university campus: economic, environmental, and sensitivity analysis, Energy Convers. Manag. X 24 (August) (2024) 100691, https://doi.org/10.1016/j.ecmx.2024.100691.
[66] Z. Qureshi, S. Ali, A. Kazmi, S. Mushtaq, M. Anwar, An integrated assessment framework of renewable based Microgrid deployment for remote isolated area electrification across different climatic zones and future grid extensions Green House gasses Internal Rate of Return, Sustain. Cities Soc. 101 (July 2023) (2024) 105069, https://doi.org/10.1016/j.scs.2023.105069.
[67] P.E. Report, D. Companies, Performance evaluation report distribution companies, Online]. Available, https://iesco.com.pk/saifi-saidi, 2022.
[68] C. H. C. & Co, “Islamabad electric supply company limited: annual report for the financial year 2024-25,” 2024.
[69] M. Prum, H. Hwang, D. Zhang, W. Dai, T. Agustiono, K. Chen, Optimizing hybrid energy systems for remote communities in Asia ’ s least developed countries, Heliyon 10 (8) (2024) e293691–22, https://doi.org/10.1016/j.heliyon.2024.e29369.
[70] S. Kwon, H. Gil, S. Baek, H. Kim, Optimal solution for a renewable-energy-generation system at a private educational institute in South Korea, Energies 14 (24) (2022) 1–11.
[71] E. Park, S.J. Kwon, A.P. Pobil, Can large educational institutes become free from grid systems ? determination of hybrid renewable energy systems in Thailand, Appl. Sci. 9 (11) (2019) 2319, https://doi.org/10.3390/app9112319.
[72] F. Ali, M. Ahmar, Y. Jiang, M. Alahmad, A techno-economic assessment of hybrid energy systems in rural Pakistan, Energy 215 (2021) 119103, https://doi.org/10.1016/j.energy.2020.119103.
[73] Z. Du, et al., Decarbonisation of data centre networks through computing power migration, in: 2025 IEEE 5th International Conference on Computer Communication and Artificial Intelligence (CCAI), IEEE, 2025, pp. 871–876, https://doi.org/10.1109/CCAI65422.2025.11189418.
[74] R. Aghamolaei, M. Fallahpour, Strategies towards reducing carbon emission in university campuses : a comprehensive review of both global and local scales, J. Build. Eng. 76 (June) (2023) 107183, https://doi.org/10.1016/j.jobe.2023.107183.
[75] S. Giannelos, I. Konstantelos, X. Zhang, G. Strbac, A stochastic optimization model for network expansion planning under exogenous and endogenous uncertainty, Electr. Power Syst. Res. 248 (May) (2025) 111894, https://doi.org/10.1016/j.epsr.2025.111894.
[76] S.O. Brien, Z. Ul, A. Qureshi, R. Aghamolaei, Comparative life cycle assessment of district heating supply pathways : insights from waste heat and CHP configurations, Results Eng. 28 (September) (2025).
[77] Z. Dong, X. Zhang, L. Zhang, S. Giannelos, G. Strbac, Flexibility enhancement of urban energy systems through coordinated space heating aggregation of numerous buildings, Appl. Energy 374 (July) (2024) 123971, https://doi.org/10.1016/j.apenergy.2024.123971.
[78] S. Giannelos, D. Pudjianto, T. Zhang, G. Strbac, Energy hub operation under uncertainty : Monte Carlo risk assessment using gaussian and KDE-based data, Energies 18 (2025) 1712.
[79] HOMER® Energy, “HOMER ENERGY version 3.7 Help Manual,” 2016.
[80] S.B. of Pakistan, Inflation monitor, Online]. Available, https://www.sbp.org.pk/publications/Inflation_Monitor/2024/Jun/IM_June_2024.pdf, 2024.
[81] M.S. Moeen, F.A. Memon, N. Hafeez, Pakistan energy outlook report 2021-2030, Pakistan Energy Outlook Rep. (March) (2022).
[82] L. Khalil, K. Liaquat, M.A. Iqbal, M. Riaz, K. Khalil, Materials today : proceedings optimization and designing of hybrid power system using HOMER pro, Mater. Today Proc. 47 (2021) S110–S115, https://doi.org/10.1016/j.matpr.2020.06.054.
[83] N. Ennemiri, A. Berrada, A. Emrani, J. Abdelmajid, R. El Mrabet, Optimization of an off-grid PV/biogas/battery hybrid energy system for electrification: a case study in a commercial platform in Morocco, Energy Convers. Manag. X 21 (October 2023) (2024) 100508, https://doi.org/10.1016/j.ecmx.2023.100508.
[84] M.Ashraful Islam, et al., Assessing the feasibility and quality performance of a renewable energy-based hybrid microgrid for electrification of remote communities, Energy Convers. Manag. X 23 (May) (2024) 100674, https://doi.org/10.1016/j.ecmx.2024.100674.
[85] E. Ayodele, S. Misra, R. Damasevicius, R. Maskeliunas, Hybrid microgrid for micro fi nance institutions in rural areas – a field demonstration in West Africa, Sustain. Energy Technol. Assessments 35 (June) (2019) 89–97, https://doi.org/10.1016/j.seta.2019.06.009.
[86] Y.K. Güven, A. Fatih, Optimization of hybrid renewable energy systems for a public hospital : a case study of grid and off-grid solutions in Yalova, 11. International European congress on advanced studies in basic sciences, Int. Eur. Congr. Adv. Stud. Basic Sci. (November) (2024).
[87] S. Yadav, P. Kumar, A. Kumar, Techno-economic assessment of hybrid renewable energy system with multi energy storage system using HOMER, Energy 297 (April) (2024) 131231, https://doi.org/10.1016/j.energy.2024.131231.

[88] D. Suganthi, K. Jamuna, Energy Conversion and Management : X Optimizing campus microgrid energy systems : economic, environmental, and sensitivity insights, Energy Convers. Manag. X 27 (April) (2025) 101046, https://doi.org/10.1016/j.ecmx.2025.101046.

[89] B. Hüner, Feasibility and environmental analysis of biogas-based hybrid energy system using HOMER pro software: a case study for Hatay, Energy Convers. Manag. 326 (November 2024) (2025) 119480, https://doi.org/10.1016/j.enconman.2025.119480.

[90] T.A. Woldegiyorgis, et al., Techno-economic feasibility analysis of a hybrid wind-PV-diesel energy system for Kiltu village, Oromia, Ethiopia using HOMER pro, Environ. Res. Commun. 7 (5) (2025) 055004, https://doi.org/10.1088/2515-7620/add242.

[91] B. Panbechi, A. Hajinezhad, S.F. Moosavian, R. Fattahi, Enhancing the enviro-economic viability of biogas-solar hybrid systems: strategies for sustainable energy development in Iran, Energy Strateg. Rev. 58 (December 2024) (2025) 101671, https://doi.org/10.1016/j.esr.2025.101671.

[92] H. Saleeb, A.M. El-Rifaie, K. Sayed, O. Accouche, S.A. Mohamed, R. Kassem, Optimal sizing and techno-economic feasibility of hybrid microgrid, Processes 13 (4) (2025) 1209, https://doi.org/10.3390/pr13041209.

[93] M.F. Ali, M.A. Halim, M.M. Julhash, M. Ashikuzzaman, Economic and environmental benefits of grid-connected PV-biomass systems in a Bangladeshi university: a HOMER Pro approach, Int. Trans. Electr. Energy Syst. 2025 (1) (2025), https://doi.org/10.1155/etep/5053853.

[94] H. Demir, Design and optimization of hybrid renewable energy systems for hydrogen production at Aksaray University campus, Process Saf. Environ. Prot. 192 (September) (2024) 543–556, https://doi.org/10.1016/j.psep.2024.10.080.

[95] N. Paltrinieri, Y. Liu, S. Ahmet, B. Barıs, O. Yoldas, Optimum sizing of hybrid renewable power systems for on-site hydrogen refuelling stations : case studies from Türkiye and Spain ¸ e Erdo g, Int. J. Hydrogen Energy 59 (October 2023) (2024) 715–729, https://doi.org/10.1016/j.ijhydene.2024.02.068.

[96] A. Al, H.A. Kanjo, M. Maurice, A. Hamid, M. Hussein, T. Salameh, Techno-economic feasibility of green hydrogen production using hybrid solar-wind energy systems in Oman, Int. J. Thermofluids 28 (June) (2025) 101302, https://doi.org/10.1016/j.ijft.2025.101302.

[97] A. El-maaroufi, M. Daoudi, R. Ahl, Hydrogen production for SDG 13 using hybrid renewables energies in southern Morocco, Energy 319 (January) (2025) 134986, https://doi.org/10.1016/j.energy.2025.134986.

[98] K. Ram, S.S. Chand, R. Prasad, A. Mohammadi, M. Cirrincione, Microgrids for green hydrogen production for fuel cell buses – A techno-economic analysis for Fiji, Energy Convers. Manag. 300 (November 2023) (2024).